ChemPubSoc Europe

https://doi.org/10.1002/ejic.201800349

EurJIC European Journal of Inorganic Chemistry

Full Paper

Tuning M–M Distances

Rhodium(I) Complexes of *N*-Aryl-Substituted Mono- and Bis(amidinates) Derived from Their Alkali Metal Salts

Eric M. B. Moos,[a] Sandra González-Gallardo,[a] Michael Radius,[a] and Frank Breher*[a]

Dedicated to Professor A. C. Filippou on the occasion of his 60th birthday

Abstract: The synthesis and characterization of several rhodium(I) complexes of amidinate and linker-bridged bis(amidinate) ligands are presented. The amidinate ligands for the mononuclear complexes $CH_3\{C(NMes)_2Rh(cod)\}$ (**1**), $CH_3\{C(NDipp)_2Rh(cod)\}$ (**2**), and $HCC\{C(NDipp)_2Rh(cod)\}$ (**3**) (cod = 1,5-cyclooctadiene) were synthesized by reacting the corresponding organometallic precursor $[Rh(cod)Cl]_2$ with the alkali metal amidinates $CH_3\{C(NR)_2Li\}$ **L1Li** (R = Mes = 2,4,6-$Me_3C_6H_2$) and **L2Li** (R = Dipp = 2,6-$iPr_2C_6H_3$). Analogously, the alkynyl-functionalized sodium amidinate ($HCC\{C(NDipp)_2Na\}\cdot 2DME$, **L3Na**) could be further deprotonated and reacted with carbodiimine to form the alkyne-bridged bis(amidinate) $CC\{C(NDipp)_2Na(thf)\}_2$ (**L4Na**), which serves as suitable starting material for the synthesis of $CC\{C(NDipp)_2Rh(cod)\}_2$ (**4**). The bis(amidinate) ligands for the corresponding *para*- (**5**) and *meta*- (**6**) phenylene-bridged complexes *p*-/*m*-$C_6H_4\{C(NMes)_2Rh(cod)\}_2$ were accessible through the reaction of phthalic acids with trimethylsilyl polyphosphate and mesitylamine and subsequent deprotonation of the obtained amidines. Tetramesityl oxalamidinate was used to synthesize the dinuclear complex $\{C(NMes)_2Rh(cod)\}_2$ (**7**) and its carbonylation product $\{C(NMes)_2Rh(CO)_2\}_2$ (**8**). All compounds under study were fully characterized by various spectroscopic methods. In particular the alkali metal salt of the linker-bridged bis(amidinate) **L5Na** forms a one-dimensional coordination polymer in the solid state. Reaction of **L5Na** and **L6Na** with $[Rh(cod)Cl]_2$ leads to dinuclear complexes in which the metal–metal distance can be adjusted, enabling us to study their reactivity, including possible cooperative effects in catalysis.

Introduction

In modern coordination chemistry, anionic amidinate ligands have attracted widespread attention in various areas, ranging from main group to rare-earth and transition metal chemistry.[1–13] However, although many transition metal complexes have been described, also including polynuclear complexes, rhodium complexes of amidinates remain scarce. So far, only five rhodium(I) complexes of amidinate ligands have been reported (**I**–**V** in Scheme 1).[14–17] In the formal oxidation state +II, two rhodium centers form paddlewheel complexes, ligated by four amidinates. Hanan et al. were able to synthesize and characterize four of such systems (**VI**–**IX**).[18] For rhodium(III), only one example of a tris(amidinato) complex (**X**) has been reported by Hursthouse et al.[19]

Focusing on rhodium(I) complexes in general, and polynuclear complexes in particular, we became interested in investigating the chemistry of linker-bridged bis(amidinates) and their bimetallic complexes. In general, amidinate units can be bridged either at their nitrogen atoms or at the carbon centers.[20] In order to access rigid systems with "tailored" metal–metal distances, we became interested in exploring the structural diversity of carbon bridged bis(amidinates). If two amidinates are linked without inserting a linker molecule, oxalic amidinates are obtained.[21,23,24] Derived from oxalic acid, these ligands favor a κ^2N coordination to form five-membered metallacycles. In case the bis(amidinates) are bridged using organic linkers,[22] the orientation of the two metals depends on the linker topology. Such a strategy offers a great potential for structurally tuning M–M distances in bimetallic complexes and

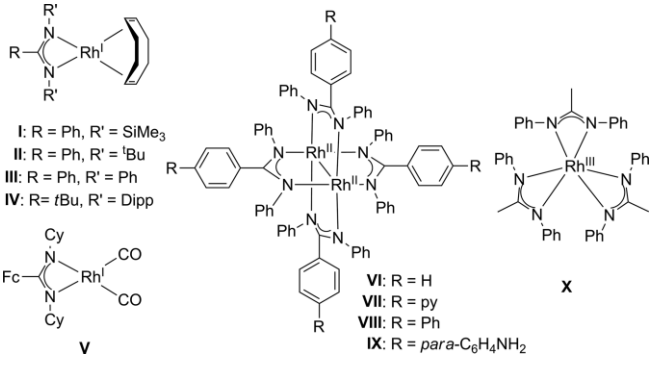

Scheme 1. Known amidinate complexes **I**–**X** from the literature.

[a] *Institute of Inorganic Chemistry, Division of Molecular Chemistry, Karlsruhe Institute of Technology (KIT), Engesserstr. 15, 76131 Karlsruhe, Germany*
E-mail: breher@kit.edu
www.aoc.kit.edu

Supporting information and ORCID(s) from the author(s) for this article are available on the WWW under https://doi.org/10.1002/ejic.201800349.

© 0000 Wiley-VCH Verlag GmbH & Co. KGaA, Weinheim

has already been successfully applied in polymerization[20,22,25] and hydroamination catalysis.[26]

Results and Discussion

Synthesis and Characterization of the Mono- and Bis(amidinates)

The alkali metal salts of the amidinate ligands were prepared using the straightforward reaction of alkali metal organyls with carbodiimines (Scheme 2).[1] The reaction of MeLi with dimesityl-carbodiimine and bis(2,6-diisopropylphenyl)carbodiimine led to the formation of the corresponding monoamidinates **L1Li** and **L2Li** in 42 % and 48 % isolated yields, respectively. The ^{1}H NMR spectrum suggests a symmetric, chelating coordination mode of the amidinate ligand in solution, since only one set of signals is observed for the mesityl and diisopropylphenyl substituents on the ligands backbones (see the Experimental Section for details). Unfortunately, the obtained crystals were not suitable for X-ray diffraction, thus no structural information in the solid state is available.

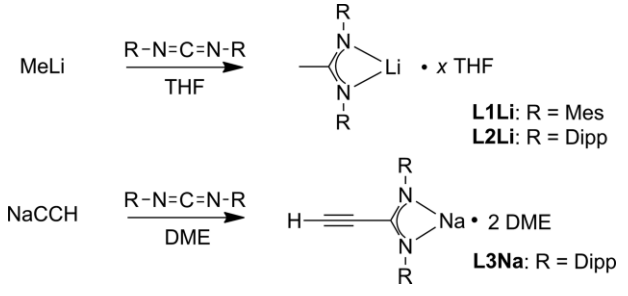

Scheme 2. Synthesis of **L1Li**, **L2Li** and **L3Na** (Mes = 2,4,6-$Me_3C_6H_2$; Dipp = 2,6-$iPr_2C_6H_3$).

The reaction of sodium acetylide with bis(diisopropylphenyl)carbodiimine in dimethoxyethane (DME) furnished the alkynyl-functionalized amidinate (**L3Na**) as a microcrystalline colorless solid in 86 % yield (Scheme 2). For the alkynyl terminated derivative, the corresponding ^{1}H NMR spectrum also suggests a symmetric κ^2N coordination mode of the amidinate ligand in solution. In addition, two signals at δ_{1H} = 3.00 and 3.08 ppm are evidence of the coordination of two molecules of DME to the sodium atom.

The anticipated coordination mode of the ligand was confirmed by the solid-state structure of **L3Na** (Figure 1). The compound crystallizes in the monoclinic $P2_1/n$ space group with one molecule in the asymmetric unit. The sodium center is coordinated by two nitrogen atoms of the amidinate ligand and four oxygen atoms, which correspond to two molecules of dimethoxyethane.

Sodium amidinates have not been investigated as extensively as their lithium or potassium congeners.[6] Among the few mononuclear sodium amidinates that have been described, the formamidinate [Na(κ^2N-FIso)(dme)$_2$] [FIso = *N*,*N*′-di(2,6-diisopropylphenyl)formamidine] bears bulky Dipp substituents and can therefore be considered as an analogue of **L3Na**.[27]

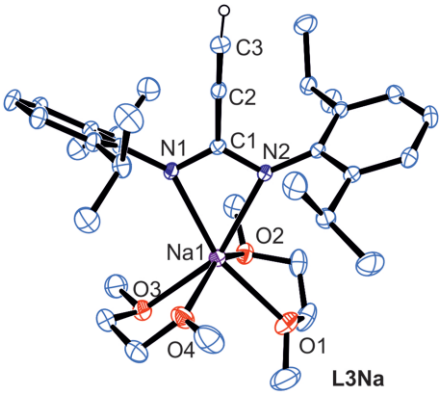

Figure 1. Molecular structure of **L3Na**; displacement ellipsoids are drawn at the 30 % probability level. H atoms (except H1) are omitted for clarity. Selected bond lengths [pm] and angles [°]: Na–N1 245.6(1), Na–N2 243.9(1), Na–O1 240.5(2), Na–O2 249.9(1), Na–O3 239.6(1), Na–O4 247.0(1), N1–C1 132.3(2), N2–C1 132.9(2), N1–C1–N2 119.3(1), N1–Na1–N2 55.7(1).

In order to synthesize the first alkyne-bridged bis(amidinate) (**L4Na**), **L3Na** was deprotonated using sodium bis(trimethylsilyl)amide and subsequently reacted with bis(diisopropylphenyl)carbodiimine in dimethoxyethane (Scheme 3).

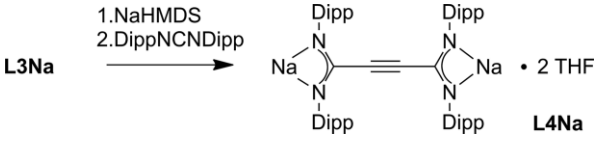

Scheme 3. Synthesis of **L4Na**.

Interestingly, the reaction did not proceed cleanly using THF as a solvent, yet no pure crystalline **L4Na** could be obtained from solutions in DME. Conducting the reaction in DME and changing the solvent to THF before layering with hexane, however, led to the formation of analytically pure **L4Na** in form of very large, slightly yellowish crystals. ^{1}H NMR spectroscopic investigations in [D$_8$]THF showed only very broad overlapping signals. Hence, spectra were acquired in C_6D_6, in which **L4Na** is barely soluble. The isopropyl protons were detected as four doublets with chemical shifts of δ_{1H} = 1.11, 1.16, 1.39 and 1.46 ppm and two septets at $\delta_{1\,H}$ = 3.57 and 3.70 ppm.

This finding, however, could be explained by inspecting the solid-state structure. **L4Na** crystallizes in the orthorhombic space group $P2_12_12_1$ with four molecules within the unit cell. The structure is shown in Figure 2; relevant bond lengths and angles are compiled in the caption. As already deduced from the NMR investigations, each sodium atom is only coordinated by one amidinate nitrogen atom [Na1–N1 232.0(2) pm, Na2–N4 232.8(2) pm], as well as by one THF molecule [Na1–O1 230.9(3) pm, Na2–O2 231.1(3) pm]. Further coordinative stabilization is provided by weak contacts to the alkynyl carbon atoms [*d*(Ø) = 302.4 pm] and the phenyl rings of the Dipp substituents [*d*(Ø) = 311.1 pm]. For the other two *exo*-oriented substituents, the N1–C_{Dipp} und N4–C_{Dipp} bonds are arranged almost parallel to the central C1–C3–C4–C2 vector. These Dipp substituents have no bonding interaction with the sodium atoms, thus leading to two chemically inequivalent types of Dipp groups within

© 0000 Wiley-VCH Verlag GmbH & Co. KGaA, Weinheim

the molecule. The retention of this structural motif in solution is consistent with the observed NMR spectra.

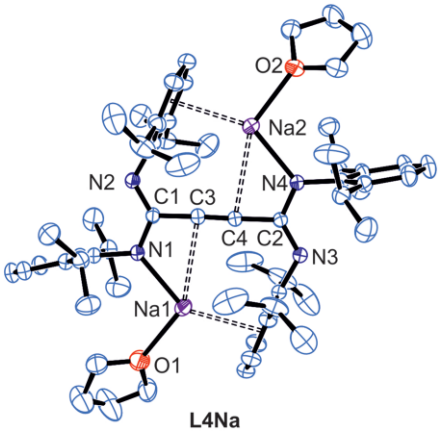

Figure 2. Molecular structure of **L4Na**; displacement ellipsoids are drawn at the 30 % probability level. H atoms are omitted for clarity. Selected bond lengths [pm] and angles [°]: C3–C4 119.9(3), Na1–N1 232.0(2), Na2–N4 232.8(2), Na1–O1 230.9(3), Na2–O2 231.1(3), Na1–C3 302.3(3), Na2–C4 302.4(3), N1–C1 132.7(3), N4–C2 132.4(3), N2–C1 130.8(3), N3–C2 131.2(3), C1–C3 145.5(3), C2–C4 145.6(3), N1–C1–N2 127.2(2), N3–C2–N4 126.9(2).

In our endeavor to provide a series of linker-bridged bis(amidinates), we also investigated *para*- and *meta*-phenylene linkers. Complexes of *p*-phenylene-bridged bis(amidinates) are already known in the literature. Although not many examples have been reported so far, some examples for main group,[20] d-block,[28] and lanthanoid complexes are known.[29] Although *m*-phenylene-bridged systems have been mentioned in a Japanese patent,[30] no metal complexes thereof have been reported so far. To synthesize the ligands, attempts to prepare $Li_2C_6H_4$ and subsequent reaction with carbodiimines were unsuccessful. However, in 2011 Lei et al. presented the successful synthesis of 2,6-diisopropylphenyl- and 2,6-dimethylphenyl-substituted derivatives of *para*-phenylene-bridged bis(amidines)[20] by using the corresponding dicarboxylic acids as starting materials. These acids were treated with PPSE (polyphosphoric acid trimethylsilyl ester) at 180 °C, forming the bridged bis(amidines).

We successfully applied this route for the synthesis of the mesityl-substituted *para*- and *meta*-phenylene-bridged bis(amidines) **L5H** and **L6H** (Scheme 4). The crude products contain large quantities of mesitylamine, which must be removed through multiple washing and crystallization steps, after which both compounds could be obtained in good yields (**L5H**: 69 %, **L6H**: 50 %).

Despite the simple structure of the amidines, their ^{1}H NMR spectra show an unexpectedly large number of very broad and overlapping signals in common deuterated solvents. A plausible explanation is aggregation in solution. In 2016, Meyer et al.[31] described the formation of linear dimers of symmetric *N*,*N*′-disubstituted amidines in solution. They were able to identify dimeric aggregates of the (*E*/*Z*, *syn*/*anti*) isomers of bulky amidines, derived through rotation and tautomerization. The bifunctional bis(amidines) **L5H** and **L6H** seem to form even more complex aggregates, as the conceivable isomers of each individual amidine moiety allow them to form oligomeric aggregates in a complicated equilibrium. Hence, the obtained

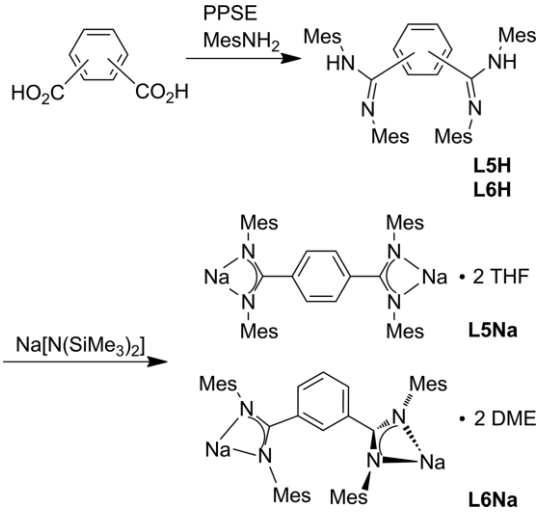

Scheme 4. Synthesis of **L5Na** and **L6Na** via their protonated analogues **L5H** and **L6 H**, respectively PPSE (polyphosphoric acid trimethylsilyl ester).

NMR spectra (see Figure S11 and S15 of the Supporting Information) may be characteristic, yet, they are not suitable for proper NMR signal-to-core-assignment using conventional methods.

Nevertheless, we were able to confirm the identity of the products, based on the determination of their solid-state structures with the aid of X-ray diffraction. **L5H** crystallizes in the monoclinic space group *C*2/*c* with half a molecule within the asymmetric unit and three solvent molecules per formula unit (Figure 3). As expected, the bond lengths and angles are very similar to *trans*-1,4-C_6H_8{$C(NDipp)_2H$}$_2$ reported by Lei.[20] Furthermore, **L5H** show no signs of aggregation in the solid state. **L6H** crystallizes in the triclinic space group $P\bar{1}$. However, the structure refinement was not successful, and therefore no further discussion of the bonding parameters is presented.

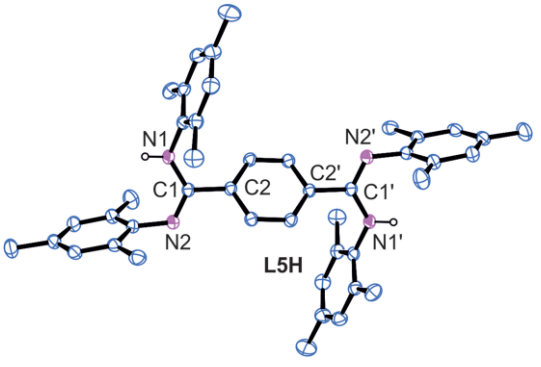

Figure 3. Molecular structure of **L5H**, displacement ellipsoids are drawn at the 30 % probability level. H atoms (except the NH entities) and solvent molecules have been omitted for clarity. Selected bond lengths [pm] and angles [°]: **L5H**: N1–C1 136.8(2), N2–C1 128.2(2), C1–C2 148.8(2), N1–C1–N2 118.5(15).

The sodium bis(amidinates) **L5Na** and **L6Na** (Scheme 4), were synthesized using the Brønsted base sodium bis(trimethylsilyl)amide in ethereal solvents. Both compounds were obtained as colorless crystals in good yields (**L5Na**: 77 %, **L6Na**: 72 %) by layering the concentrated reaction mixtures with hexane.

© 0000 Wiley-VCH Verlag GmbH & Co. KGaA, Weinheim

Notably, a filtration prior to crystallization was required, as otherwise yellowish crude powders were obtained.

In contrast to those of the precursor amidines, the ^{1}H NMR spectra of **L5Na** and **L6Na** showed single, separated signal sets, suggesting that they are monomeric in solution. It has to be noted that the spectra of **L5Na** were obtained in [D_8]THF, whereas those of **L6Na** were obtained in [D_6]DMSO, in order to avoid overlapping signals of the product and the solvent that would prevent accurate signal assignment. For that reason, no comparison between the chemical shifts of both complexes is made.

The obtained crystals of **L5Na** were suitable for X-ray diffraction, hence a solid-state structure could be obtained. The product crystallizes in the tetragonal space group $P4_2/nbc$ with a quarter of a formula unit within the asymmetric unit. In contrast to the respective amidine **L5H**, the disodium salt forms a one-dimensional coordination polymer (Figure 4) with two sodium atoms between two neighboring amidinate moieties of two adjacent bis(amidinates) and two polymer strains per unit cell. The sodium–sodium distance is 258.7(4) pm and the Na–N bond length is 266.8(3) pm. Each sodium atom is further coordinated by one THF molecule. Regarding the phenylene backbone, each moiety is tilted by 91.4° relative to the neighboring moiety. The N1–C1 bond length and the N–C–N angle differ only slightly from those of **L5H**, and the C1–C2 bond length [148.6(5) pm] is almost the same [d(C1–C2): **L5H**: 148.6 pm; **L6H**: 148.8 pm]. Overall, there is only little deviation of the structural parameters of **L5Na** as compared with the free amidine **L5H**.

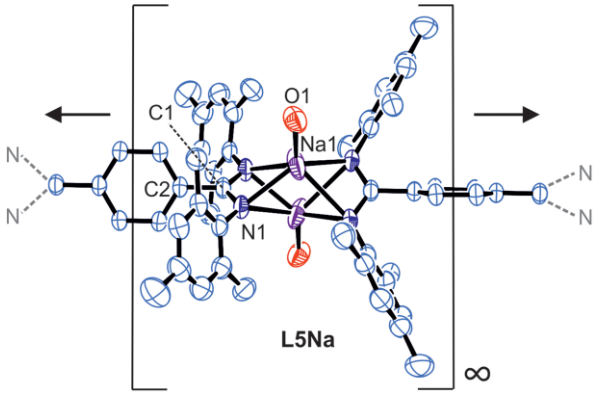

Figure 4. Section of the molecular structure of **L5Na**; displacement ellipsoids are drawn at the 30 % probability level. Hydrogen atoms and the carbon atoms of the THF molecules have been omitted for clarity. Selected bond lengths [pm] and angles [°]: Na1–Na1′ 258.7(4), Na1–O1 223.7(5), Na1–N1 266.8(3), N1–C1 133.3(3), C1–C2 148.6(5), N1–C–N1′ 116.9(3). The symmetry equivalent atoms are generated by 1/2 – *x*, 1/2 – *y*, *z*; 1/2 – *x*, *y*, 1 – *z* and *x*, 1/2 – *y*, 1 – *z*.

Regarding the *meta*-phenylene bridged **L6Na**, no crystals suitable for structure determination could be obtained. Although the compound crystallizes readily, the crystals were not suitable for X-ray diffraction. It can be expected that **L6Na**, similar to **L5Na**, forms a coordination polymer, but the periodical arrangement of the polymer is impaired by the angled nature of the *meta*-phenylene backbone.

To be able to study a comprehensive variety of bridged bis(amidinate) ligands, oxalic amidinates were also targeted. Oxalic amidines and amidinates are long known within the literature.[32] By exchanging the oxygen atoms by nitrogen atoms, they can be derived from oxalic acid. Furthermore, amidinates are able to coordinate orthogonally to the central C–C axis, preferably using the widest of the two possible donor chelate functions, similarly to what has been observed for oxalates.[33] Owing to the close spatial proximity of two metals centers in such complexes, and the four nitrogen atoms being incorporated in one small π-system, bimetallic complexes of such ligands could possess unusual properties.[24,34] Rhodium complexes of oxalic amidinates have, however, not yet been described.

The tetramesityl oxalic amidine used in this work has already been utilized by Walther et al. for the synthesis of di- and oligonuclear complexes of nickel, palladium and zinc.[21,24] Synthetic details, however, were not given. The synthesis proceeds starting from oxalyl chloride that is reacted with mesitylamine to form the oxalic amide **L7a**, following the procedure reported by Zhang et al.[35] The latter was chlorinated with PCl_5 forming the oxalic imidoyl chloride **L7b** that was treated with mesitylamine to form the target structure **L7H** using a modified version of the synthesis of tetraphenyl oxalamidine, published by Bauer in 1907 (Scheme 5).[32] Synthetic and spectroscopic data is listed in the experimental section.

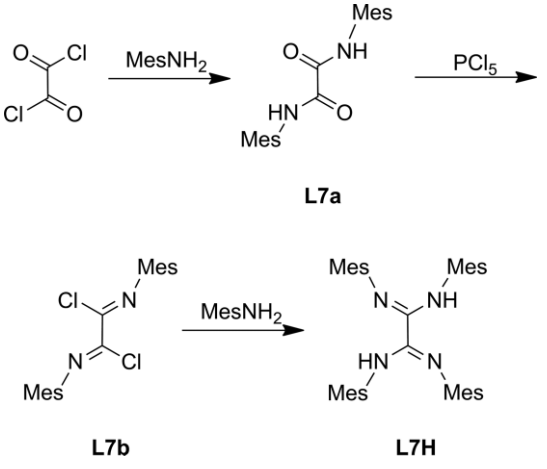

Scheme 5. Synthesis of **L7H**.

Synthesis and Characterization of the Rhodium(I) Complexes

The synthesis of the rhodium complexes was achieved through reaction of the alkali metal amidinates (Scheme 6) and bis(amidinates) (Scheme 7) with [Rh(cod)Cl]$_2$. The reactions were conducted using THF as solvent.

Interestingly, Jones et al. showed that the Dipp-substituted rhodium amidinate **IV** (see Introduction) and analogous guanidinates initially form complexes in which the rhodium is coordinated to one of the phenyl rings and only switch to κ^2N coordination upon heating to 80 °C in toluene.[16] This behavior was not observed for all of the title complexes, possibly because THF was used as solvent (except for **3**, toluene), or because Jones et al. used potassium amidinates, whereas we chose lith-

© 0000 Wiley-VCH Verlag GmbH & Co. KGaA, Weinheim

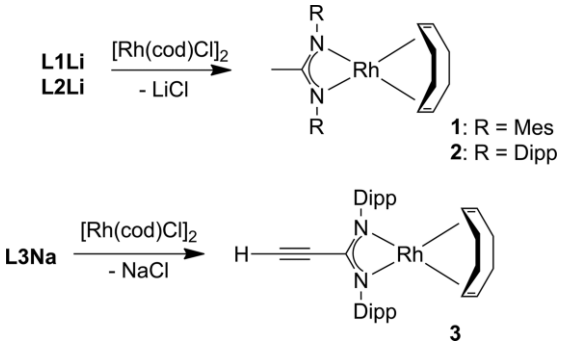

Scheme 6. Synthesis of the mononuclear rhodium(I) complexes **1**–**3**.

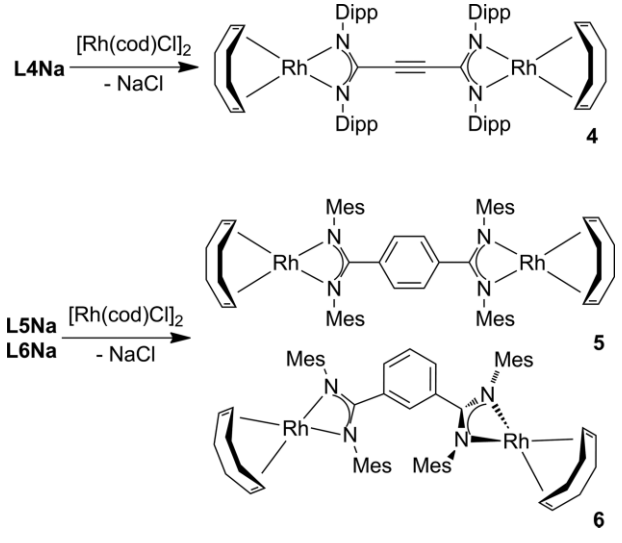

Scheme 7. Synthesis of the dinuclear rhodium(I) complexes **4**–**6**.

ium and sodium derivatives. After filtration the crude reaction mixtures were purified by crystallization. The mono-amidinate complexes **1**–**3** were obtained in good to moderate yields (**1**: 55 %, **2**: 35 %, **3**: 37 %), and are soluble in organic solvents, which simplified the acquisition of NMR spectra. In contrast, the pure bis(amidinates) complexes **4**–**7** are poorly soluble in common organic solvents, thus requiring time-consuming NMR experiments. With the exception of **4** (30 %) the bis(amidinates), however, all could be obtained in good yields (**5**: 68 %, **6**: 51 %, **7**: 77 %). During the synthesis and attempts of crystallization of **4**, formation of large amounts of an unidentified dark solid was observed. Nevertheless, pure **4** could be obtained by storing a toluene/Et_2O solution at –35 °C for several weeks and washing the precipitated red crystals with additional Et_2O. As the yields of **3** and **4** reproducibly fall out of the range found for the other derivatives, we hypothesized that significant side reactions occur, which may involve bond formation between the amidinate nitrogen atoms with the alkyne carbon atoms. Especially for **3**, which features a terminal alkyne moiety, previous reports by Cowley and co-workers suggest that the decomposition path might involve Rh^I alkyne complexes, Rh^{III} alkynyl-hydrides and/or Rh^I vinylidene complexes, which are formed by coordination of the Rh center to the C≡C bond, with subsequent oxidative addition of the terminal alkyne C–H bond and/or a hydrogen shift.[36,37] However, we were yet not able to identify any by-products.

The NMR spectroscopic investigations of **1**–**6** were performed in deuterated benzene. Although the bis(amidinate) complexes **4**–**6** proved to be barely soluble, all proton resonances and almost all carbon resonances could be detected. Selected ^1H NMR spectra of the dinuclear rhodium(I) complexes **5** and **6** are presented in Figure 5. More details are given in the Experimental Section.

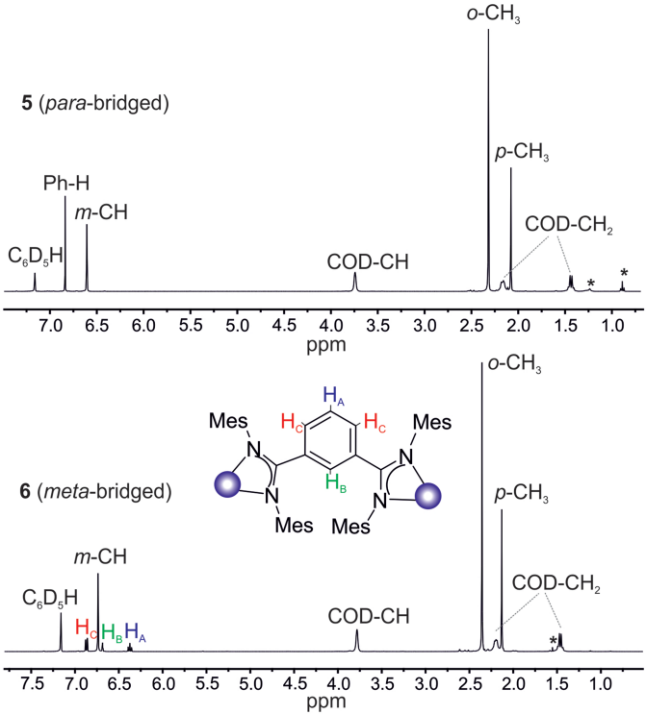

Figure 5. ^1H NMR spectra of the *m*- and *p*-phenylene-bridged bis(amidinate)-rhodium(I) complexes **5** and **6** in C_6D_6. Impurities are marked with an asterisk.

The mesityl-substituted complexes **1**, **5**, and **6** show only one set of signals for the proton resonances of the substituents; all values show only minor deviations. Only for the Dipp substituted systems **2**–**4** an evident shift can be observed, i.e. comparing the Dipp methyl resonances of the mono(amidinate) complexes **2** (δ_{1H} = 1.31, 1.48 ppm) and **3** (δ_{1H} = 1.47, 1.50 ppm) with the alkynyl-bridged bis(amidinate) **4** (δ_{1H} = 1.03, 1.52 ppm). Also, the central amidinate carbon atom ^{13}C NMR resonance for **4** (δ_{13C} = 159.0 ppm) falls out of the region of values detected for the other compounds (ca. 176.8–180.2 ppm). However, the values of carbon-rhodium coupling constants are similar for **1**–**6** (J_{CRh} = 5.1–5.6 Hz). Evidence for the coordination of the cod ligands is given by the respective ^{13}C NMR shifts of the cod-CH carbon atoms, that could be observed in form of doublets (δ_{1H} = 77.8–80.0 ppm) with J_{CRh} of 12.7–13.0 Hz, which is consistent with previous reports.[14,16] Thus, all spectroscopic data lead to the conclusion that the expected square-planar κ^2N-coordination of the {Rh(cod)} moieties is present in solution.

We were able to obtain single crystals suitable for X-ray diffraction of all rhodium(I) complexes (Figures 6 and 7, Table 1). **1** crystallizes in the orthorhombic space group *Pbca*, **2** in the

© 0000 Wiley-VCH Verlag GmbH & Co. KGaA, Weinheim

monoclinic space group *C*2/*c*, both with one molecule per asymmetric unit. **3** crystallizes from toluene in the triclinic space group $P\bar{1}$ with 0.5 molecules of toluene in the asymmetric unit. **4** crystallizes in the triclinic space group –1 with one molecule and one molecule Et_2O in the asymmetric unit. **5** and **6** crystallize in the monoclinic space groups $P2_1/c$ and $P2_1/n$ with one molecule per asymmetric unit, each.

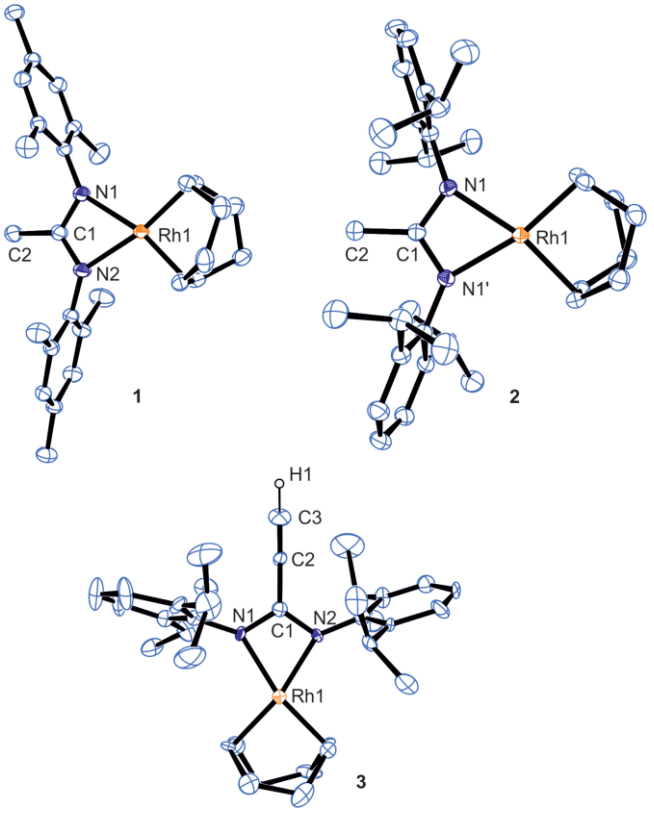

Figure 6. Molecular structures of the mononuclear rhodium(I) complexes **1**–**3**; displacement ellipsoids are drawn at the 30 % probability level. Hydrogen atoms (except H1 in **3**) and in **3** solvent molecules have been omitted for clarity. Selected bond lengths [pm] and angles [°] are given in Table 1. The symmetry equivalent atoms of **2** are generated by $-x + 1, y, -z + 1/2$.

All crystal structures confirmed the anticipated slightly distorted square-planar coordination environment for the rhodium centers upon symmetrical *N*,*N*′-coordination of the respective amidinate ligand and one η^2,η^2-1,5-cyclooctadiene ligand.

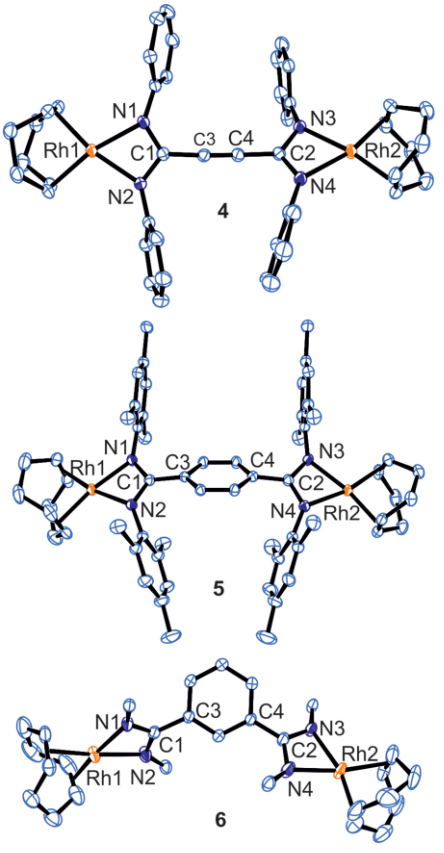

Figure 7. Molecular structures of the dinuclear rhodium(I) complexes **4**–**6**; displacement ellipsoids are drawn at the 30 % probability level. Hydrogen atoms have been omitted for clarity. Selected bond lengths [pm] and angles [°] are given in Table 1. In **4** isopropyl groups and solvent molecules are omitted, in **6** mesityl substituents are reduced to *ipso* carbon atoms for clarity.

Owing to the intrinsically high rigidity of the amidinates, only minor deviations regarding the structural parameters were observed, with the exception of **2**, for which the coordination of the rhodium center is less symmetrical. Here, one rhodium–nitrogen bond [Rh1–N1 204.4(9) pm] is significantly shorter than the other [Rh1–N2 211.8(8) pm] and the respective N–C bonds towards the central C1 atom differ even more [N1–C1 126.1(2), N2–C1 139.2(6) pm]. Thus, the rhodium center in **2** is not coordinated as symmetrically as in the other complexes,

Table 1. Selected bond lengths [pm] and angles [°] of rhodium complexes **1**–**6**.

	1	**2**	**3**	**4**	**5**	**6**
Rh1–C1	251.4(2)	251.5(3)	253.8(5)	253.9(3)	253.3(3)	252.8(3)
Rh1–N1	210.04(18)	208.33(16)	212.0(4)	210.3(3)	209.4(3)	208.7(3)
Rh1–N2	207.67(18)	–	208.6(4)	209.9(3)	208.8(3)	210.0(3)
Rh2–C2	–	–	–	253.6(3)	253.2(3)	252.4(3)
Rh2–N3	–	–	–	208.0(3)	209.0(3)	208.7(3)
Rh2–N4	–	–	–	211.9(3)	207.8(3)	208.9(3)
C1–N1	132.9(3)	132.3(2)	134.5(6)	131.8(4)	133.4(4)	132.7(5)
C1–N2	132.2(3)	–	132.9(6)	132.8(4)	132.7(4)	132.2(5)
C2–N3	–	–	–	133.9(4)	133.6(4)	132.4(4)
C2–N4	–	–	–	131.9(4)	132.7(4)	131.8(5)
N1–C1–N2	111.80(19)	111.7(2)	111.5(4)	111.0(3)	110.9(3)	111.4(3)
N3–C2–N4	–	–	–	111.4(3)	110.5(3)	111.4(3)

© 0000 Wiley-VCH Verlag GmbH & Co. KGaA, Weinheim

with N1 having a more imine character and N2 acting more like an amide. However, this behavior seems to be limited to the solid state since the above described NMR investigation did not show inequality of the substituents, hence, all other collected structural parameters are in good agreement with literature values.[14–16] The rhodium–rhodium distances within the bis(amidinates) rise from the alkynyl-bridged **4** (917.9 pm) over the *m*-phenylene-bridged **6** (964.1 pm) to the *p*-phenylene-bridged **5** (1069.3 pm).

Since our studies on linker-bridged rhodium bis(amidinates) should also include the "non-linker" bis(amidinates), we used the above mentioned oxalamidine **L7H** in reactions with rhodium precursors. To synthesize the dinuclear rhodium oxalic amidinate complex **7**, we reacted **L7H** with $[Rh(cod)Cl]_2$ and $Na[N(SiMe_3)_2]$ in toluene. The reaction does not proceed cleanly and **7** precipitates in form of a yellow powder from a dark brown solution. However, **7** is almost insoluble in all common solvents, thus purification could be easily achieved by vigorous washings with CH_2Cl_2 and water (yield: 61 %).

The insolubility of **7** impedes its characterization in solution, and thus satisfactory NMR spectra could only be obtained with long-term measurements. As expected, the ^{1}H NMR spectrum indicates a symmetric molecule with only one set of signals for the substituents and the cod co-ligands (Figure 8). In contrast to the rhodium bis(amidinates) **4**–**6**, the proton resonances of the cod ligands in **7** are significantly shifted to lower frequencies. This can likely be attributed to the different coordination environment of the rhodium atoms in oxalic amidinate complexes, as compared to the aforementioned amidinates.

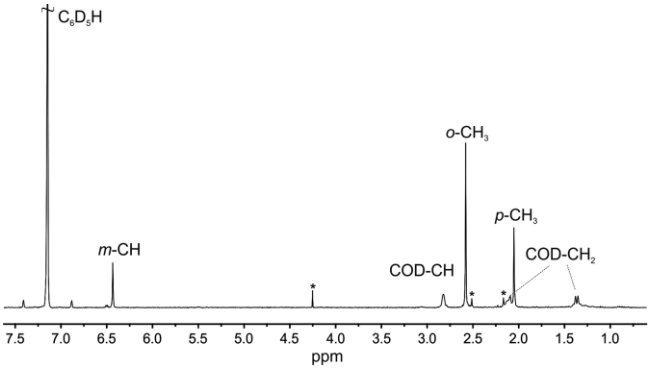

Figure 8. ^{1}H NMR spectrum of **7** in C_6D_6. Impurities are marked with an asterisk.

Crystals suitable for X-ray diffraction were obtained, further confirming the identity of **7** (space group *C*2/*c*, with half a molecule and one molecule of THF, as well as half a molecule of benzene in the asymmetric unit). The structure (Figure 9) shows the two rhodium atoms (Rh1···Rh1: 566.6 pm) to be embedded in the perfectly planar oxalic amidinate scaffold, forming two five-membered metallacycles. This topology indicates some kind of delocalization of the π-electrons over the complete unit. The square-planar coordination is completed by the cod co-ligands. As can be expected, the angle N1–C1–N2 around the connected amidinate moieties of 130.7(2)° is comparably larger than in the rhodium bis(amidinates) (**4**–**6** Ø = 110.9°), which coordinate forming a four-membered ring.

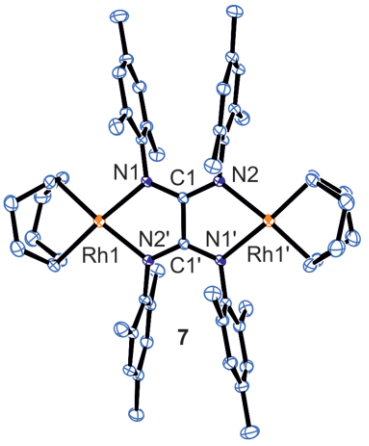

Figure 9. Molecular structures of **7**; displacement ellipsoids are drawn at the 30 % probability level. Hydrogen atoms have been omitted for clarity. Selected bond lengths [pm] and angles [°]: C1–C1′1.521(5), N1–C1 1.329(4), N2–C1 1.327(4), Rh1–N1 2.093(2), Rh1–N2′ 2.089(2), N1–C1–N2 130.7(2), N1–C1–C1′ 114.4(3), N2–C1′–C1 114.9(3). The symmetry equivalent atoms are generated by 1 – *x*,1 – *y*,1 – *z*.

Interestingly, upon exposure to CO gas, **7** reacts to form the very soluble complex **8** (Scheme 8). The reaction was conducted by applying a pressure of 2 bar of carbon monoxide onto a degassed suspension of **7** in toluene in a pressure-sealed tube and heating the mixture up to 70 °C. After stirring for two hours and drying in vacuo, pure **8** can be obtained in 95 % yield in form of a yellow powder. Owing to its good solubility, all ^{1}H and ^{13}C NMR signals could be observed and assigned with the aid of 2D correlation methods. The proton resonances of the mesityl substituents show only a small influence of the coligand, as compared to **7** [δ_{1H} **8** (**7**): *ortho*-CH_3: 2.52 (2.59), *para*-CH_3: 2.02 (2.06), Mes-CH: 6.43 (6.45) ppm]. The carbonyl carbon atoms were detected as doublet at δ_{13C} = 184.9 ppm with a rhodium coupling of $^1J_{CRh}$ = 67.3 Hz. These values are common for κ^2*N*-$Rh(CO)_2$ compounds and differ only slightly from the values for the ferrocenyl-substituted rhodium amidinate (**V**, see Introduction) reported by Arnold et al. (δ_{13C} 188.4 ppm, $^1J_{CRh}$ = 67.1 Hz).[17] The oxalic amidinates central carbon atoms were expected to be observed in form of a doublet of doublets, but were found in form of a pseudo-triplets at δ = 171.0 ppm with a coupling constant of J_{CRh} = 1.2 Hz.

Single crystals suitable for X-ray diffraction were obtained by layering a solution of **8** in benzene with hexane. **8** crystallizes in the triclinic space group $P\bar{1}$ with two independent half mol-

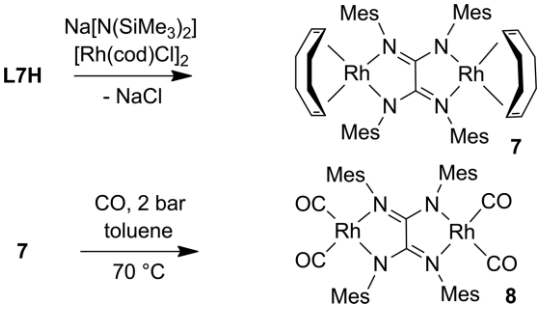

Scheme 8. Synthesis of **7** and **8**.

© 0000 Wiley-VCH Verlag GmbH & Co. KGaA, Weinheim

ecules in the asymmetric unit (Figure 10) with their oxalic amidinate planes enclosing an angle of 83.6°. The two independent molecules differ only slightly from each other. In comparison with the precursor **7**, only minor structural changes of the ligand can be observed. For the carbonyl ligands mean carbon–rhodium distances Ød(Rh–C_{CO}) = 185.4 pm and C≡O triple bond lengths of Ød(C_{CO}–O) = 113.5 pm were observed. The mean distance between the rhodium atoms and closest central oxalic amidinate atom is 288.2 pm and therefore differs from the mean value for the rhodium bis(amidinates) **4**–**6** [Ød(Rh–$C_{amidinate}$) = 253.2 pm] by 35 pm. This increase in distance nicely fits the lower J_{CRh} coupling constants in the ^{13}C NMR spectra. The CO bands in the IR spectrum are detected at 2004 and 2060 cm^{-1}.

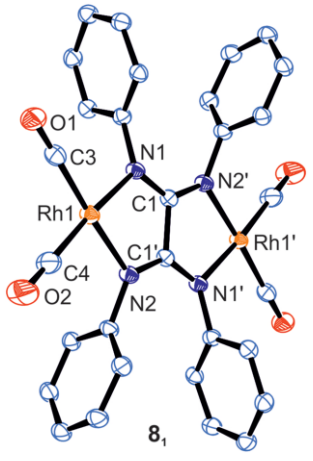

Figure 10. Molecular structure of **8**; displacement ellipsoids are drawn at the 30 % probability level. Hydrogen atoms and the methyl groups of the mesityl substituents have been omitted for clarity. Only one of the two independent molecules is shown in the Figure. Selected bond lengths [pm] and angles [°]: $\mathbf{8_1}$: C1–C1′ 151.8(5), Rh1–N1 206.0(2), Rh1–N2 205.2(3), N1–C1 131.9(4), N2–C1′ 132.2(4), Rh1–C3 185.7(3), Rh1–C4 185.3(4), C3–O1 113.5(4), C4–O2 130.0(5), N1–C1–N2′ 130.6(3). $\mathbf{8_2}$: C1–C1′ 152.0(5), Rh1–N1 206.0(2), Rh1–N2 205.1(2), N1–C1 131.6(4), N2–C1′ 131.9(4), Rh1–C3 185.4(4), Rh1–C4 185.3(4), C3–O1 113.9(5), C4–O2 113.7(4), N1–C1–N2′ 130.8(3). The symmetry equivalent atoms are generated by *–x*, *–y*, *–z* and *–1 – x*, *–y*,*1 – z*.

Conclusions

In this work we have described the synthesis and characterization of alkali metal salts of mono- and bis(amidinates), which show a rich structural diversity in the solid state. These salts, partly containing alkynyl- as well as *m*- and *p*-phenylene-bridges, can be readily employed in salt metathesis reactions by using common transition metal precursors such as $[Rh(cod)Cl]_2$ to provide several mono- and dinuclear rhodium(I) complexes, all of which comprise four-membered metallacycles and κ^2N-coordinated amidinates. The metal–metal distances can thus be adjusted, which is of interest for reactivity studies, also in the area of cooperative effects in catalysis.[38] The corresponding oxalamidinate complexes, however, were found to form five-membered metallacycles. Furthermore, we could show that the cyclooctadiene ligand present in these complexes can be substituted by CO. Studies in our laboratory continue to explore these and related types of bimetallic complexes.

Experimental Section

General Methods and Instrumentation: All manipulations were carried out using standard Schlenk line and dry-box techniques under dry argon. Methylene chloride and acetonitrile were freshly distilled under argon from calcium hydride. Toluene, diethyl ether, dme and tetrahydrofuran were dried using sodium/benzophenone ketyl. CH_2Cl_2 was distilled using CaH_2 as a drying agent. [D_8]THF and C_6D_6 were vacuum transferred from potassium/benzophenone into thoroughly dried glassware equipped with Young Teflon-valves. [D_6]DMSO was dried with CaH_2 and stored over molecular sieves (4 Å). Dimesitylcarbodiimine[39] was synthesized using literature methods. **L7a**, **L7b L7H** were synthesized by adjusted literature procedures,[32,34] described below. The $[Rh(cod)Cl]_2$ employed was obtained from commercial sources and recrystallized from CH_2Cl_2/Et_2O prior to use. Mesitylamine (2,4,6-trimethylaniline) was degassed in vacuo and distilled into a Schlenk tube containing molecular sieves (4 Å). All other reagents were used without further purification. ^1H and ^{13}C spectra were recorded on Bruker AV 300 and 400 spectrometers in dry deuterated solvents. The chemical shifts are expressed in parts per millions and ^1H and ^{13}C signals are given relative to TMS. Coupling constants *J* are given in Hertz as positive values regardless of their real individual signs. The multiplicity of the signals is indicated as s, d, q, sept or m for singlets, doublets, quartets, septets or multiplets, respectively. The assignments were confirmed as necessary with the use of 2D NMR correlation experiments. IR spectra were measured on a Bruker Alpha spectrometer using the attenuated total reflection (ATR) technique on powdered samples, and the data are quoted in wavenumbers (cm^{-1}). The intensity of the absorption band is indicated as vw (very weak), w (weak), m (medium), s (strong), vs. (very strong) and br (broad). Elemental analyses were carried out in the institutional technical laboratories of the Karlsruhe Institute of Technology (KIT). For the complex **3** the presented result is slightly outside the range viewed as establishing analytical purity. This is due to the air- and moisture-sensitive nature of the compound. However, they are provided to illustrate the best values obtained to date.

Preparation of the Compounds

Ligands

L1Li: 557 mg bis(mesityl)carbodiimide (1 equiv., 2.00 mmol) were dissolved in 20 mL of THF and cooled in an 2-propanol/$N_{2(l)}$ bath. 1.25 mL methyllithium solution (1.6 M in Et_2O, 1 equiv., 2.00 mmol) were added dropwise and the mixture was stirred overnight, allowing it to warm to room temperature. The reaction proceeds almost cleanly and simple evacuating to dryness and washing with hexane generates the product in high yields, pure enough for most applications. For further purification **L1Li** can be crystallized by layering the reduced solution (ca. 3 mL) with 9 mL of hexane. Yield after crystallization: 311 mg (0.835 mmol, 42 %). ^1H NMR (400.1 MHz, 298 K, [D_8]THF): δ = 1.13 (s, 3 H, CH_3CN_2), 2.11 (s, 12 H, *para* CH_3), 2.15 (s, 6 H, *ortho* CH_3), 6.69 (s, 4 H, mesityl CH) ppm. ^{13}C NMR (100.6 MHz, 298 K, [D_8]THF): δ = 15.5 (s, 1 C, CH_3CN_2), 19.5 (s, 4 C, *ortho* CH_3), 21.1 (s, 2 C, *para* CH_3), 128.7 (s, 2 C, *ipso* C), 128.9 (s, 4 C, *meta* CH), 132.0 (s, 4 C, *ortho* CCH_3), 150.9 (s, 2 C, *para* CCH_3), 167.0 (s, 1 C, CN_2) ppm. IR (ATR, $\tilde{\nu}$): $\tilde{\nu}$ = 444 (s), 506 (vs), 538 (vs), 563 (vs), 589 (m), 630 (m), 702 (w), 718 (w), 746 (w), 831 (w), 853 (vs), 944 (w), 976 (w), 1006 (w), 1152 (w), 1219 (vs), 1298 (w), 1373 (m), 1402 (s), 1429 (s), 1470 (vs), 1509 (s), 1608 (vw), 1645 (vw), 2728

© 0000 Wiley-VCH Verlag GmbH & Co. KGaA, Weinheim

(vw), 2855 (vw), 2915 (vw), 2957 (vw), 2994 (vw) cm^{-1}. Elemental analysis (calcd.) [%]: C: 77.57 (77.39), H: 8.22 (8.93), N: 8.99 (7.52).

L2Li: 1.50 g bis(diisopropylphenyl)carbodiimine (1 equiv., 4.14 mmol) were dissolved in 20 mL THF and cooled in an 2-propanol/$N_{2(l)}$ bath. 2.80 mL methyllithium solution (1.6 M in Et_2O, 1.1 equiv., 4.48 mmol) were added dropwise and the mixture was stirred overnight, allowing it to warm to room temperature. The reaction proceeds almost cleanly and simple evacuating to dryness and washing with hexane generates the product in high yields, pure enough for most applications. For further purification **L2Li** can be crystallized by mixing the reduced solution (ca. 7 mL) with 20 mL of hexane and storing it in the fridge (–35 °C) overnight. Yield after crystallization: 907 mg (1.99 mmol, 48 %). As for **L1Li**, the drying of the reaction mixture, followed by washing the solid with hexane yields a product pure enough for most applications. ^{1}H NMR (400.1 MHz, 298 K, [D_8]THF): δ = 1.09 (d, ^3J = 6.8 Hz, 12 H, Dipp CH_3) 1.11 (d, ^3J = 6.8 Hz, 12 H, Dipp CH_3) 1.19 (s, 3 H, N_2CCH_3), 3.54 (m, overlapped by THF, 4 H, Dipp $CHCH_3$), 6.73 (dd, J = 8.0, J = 7.1 Hz, 2 H, *para* CH), 6.90 (d, J = 7.5 Hz, 4 H, *meta* CH) ppm. ^{13}C NMR (100.6 MHz, 298 K, [D_8]THF): δ = 17.0 (s, 1 C, N_2CCH_3), 26.5, 26.6 (2s, 8 C, Dipp CH_3), 28.4 (s, 4 C, Dipp $CHCH_3$), 121.6 (s, 2 C, *para* CH), 123.1 (s, 4 C, *meta* CH), 143.0 [s, 4 C, $CCH(CH_3)_2$], 150.7 (s, 2 C, *ipso* C), 168.3 (s, 1 C, N_2C) ppm. IR (ATR, $\tilde{\nu}$): $\tilde{\nu}$ = 434 (s), 484 (m), 528 (m), 560 (w), 674 (w), 747 (w), 763 (s), 783 (m), 830 (w), 857 (vw), 894 (w), 934 (w), 960 (w), 1045 (m), 1099 (w), 1190 (w), 1208 (w), 1241 (s), 1315 (s), 1360 (m), 1381 (m), 1412 (s), 1433 (vs), 1461 (vs), 1492 (vs), 1588 (vw), 1640 (w), 2866 (w), 2917 (w), 2957 (s), 3016 (vw), 3049 (vw) cm^{-1}. Elemental analysis (calcd.) [%]: C: 79.60 (78.91), H: 9.87 (9.93), N: 5.82 (6.13).

L3Na: Sodium acetylide (1 g, 0.020 mol) was suspended in dimethoxyethane (10 mL) and a solution of bis(diisopropylphenyl)-carbodiimine (6.6 g, 0.018 mmol) in DME (50 mL) was added dropwise. The reaction mixture was stirred for 18 h. After filtration, all volatiles were evaporated in vacuo to leave a white solid, which was washed with pentane (20 mL), filtered and dried in vacuo. Yield: 9.2 g (86 %). ^{1}H NMR (300 MHz, 298 K, C_6D_6): δ = 1.37 [d, $^3J_{HH}$ = 6.84 Hz, 12 H, $CH(CH_3)_2$], 1.56 [d, $^3J_{HH}$ = 6.84 Hz, 12 H, $CH(CH_3)_2$], 1.95 (s, 1 H, C≡*CH*), 3.00 [s, 12 H, $(CH_2OCH_3)_2$], 3.08 [s, 8 H, $(CH_2OCH_3)_2$], 3.79 [sept, $^3J_{HH}$ = 6.84 Hz, 4 H, $CH(CH_3)_2$], 7.18 (m, 2 H, *p*-Ar-*H*), 7.30 ppm (m, 4 H, *m*-Ar-*H*). ^{13}C NMR (75 MHz, 298 K, C_6D_6): δ = 23.8 [$CH(CH_3)_2$], 24.6 [$CH(CH_3)_2$], 28.0 [$CH(CH_3)_2$], 58.3 [$(CH_2OCH_3)_2$], 67.5 [$(CH_2OCH_3)_2$], 79.7 (C≡*CH*), 121.5 (*p*-Ar-*C*), 122.4 (*m*-Ar-*C*), 142.4 (*o*-Ar-C_{ipso}), 149.5 ppm (Ar-C_{ipso}-N). IR (ATR, $\tilde{\nu}$): $\tilde{\nu}$ = 430 (vw), 641 (m), 699 (w), 766 (m), 855 (w), 1087 (vs), 1193 (w), 1244 (w), 1314 (w), 1428 (m), 1487 (vs), 2082 (vw), 2228 (vw), 2864 (w), 2927 (w) 2957 (w), 3260 (w) cm^{-1}. EI/MS: *m/z* (%) = 410.45 (15.18) $[M - 2dme]^+$; m.p. 155 °C (dec.). Elemental analysis (calcd.) [%]: C 71.15 (73.87), H 9.38 (9.93), N 4.74 (4.53).

L4Na: 1.489 g L**3Na** (1 equiv., 2.52 mmol) and 0.463 g Na[$N(SiMe_3)_2$] (0.9 equiv., 2.52 mmol) stirred in 30 mL DME for 3 h. To the yellow solution 0.913 g bis(diisopropylphenyl)carbodiimide in 25 mL DME were added and stirred overnight. The reaction mixture was dried in vacuo and the solvent changed to 45 mL of THF. The mixture was quickly filtered through a syringe filter and immediately layered with 60 mL of hexane. Within a few weeks, **L4Na** forms very large slightly yellowish crystals which are filtered off, washed with 10 mL of hexane and dried in vacuo (1.450 g, 1.54 mmol, 61 %). ^{1}H NMR (400.1 MHz, 298 K, C_6D_6): δ = 1.11 (d, ^3J = 6.9 Hz, 12 H, Dipp CH_3), 1.16 (d, ^3J = 6.7 Hz, 12 H, Dipp CH_3), 1.35 (m, THF CH_2), 1.39 (d, ^3J = 6.7 Hz, 12 H, Dipp CH_3), 1.46 (d, ^3J = 7.0 Hz, 12 H, Dipp CH_3), 3.41 (m, THF CH_2), 3.57 [m, 4 H, Dipp $CH(CH_3)_2$], 3.70 [m, 4 H, Dipp $CH(CH_3)_2$], 6.50 (t, ^3J = 7.5 Hz, 2 H, Dipp CH), 6.93 (q, ^3J = 7.5 Hz, 5 H, Dipp CH), 7.12 (m, 2 H, Dipp CH), 7.24 (m, 3 H, Dipp CH) ppm. ^{13}C NMR (100.6 MHz, 298 K, C_6D_6): δ = 23.5 (s, 2 C, Dipp CH_3), 23.8 (s, 2 C, Dipp CH_3), 24.7 (s, 2 C, Dipp CH_3), 25.0 (s, 2 C, Dipp CH_3), 25.6 (2S, THF CH_2), 27.8 [s, 2 C, $CH(CH_3)_2$], 28.4 [s, 2 C, $CH(CH_3)_2$], 67.9 (s, THF CH_2), 119.8 (s, Dipp CH), 121.9 (s, Dipp CH), 122.8 (s, Dipp CH), 122.8 (s, Dipp CH), 123.0 (s, Dipp CH), 127.4 (s, Dipp CH), 128.7 (s, Dipp C_{quart}), 141.5 (s, Dipp C_{quart}), 144.5 (s, Dipp C_{quart}), 148.0 (s, Dipp C_{quart}), 148.5 (s, Dipp C_{quart}), 149.6 (s, Dipp C_{quart}) ppm. The alkyne carbon resonances could not be detected. IR (ATR, $\tilde{\nu}$): $\tilde{\nu}$ = 405 (w), 431 (vw), 551.8 (vw), 671 (vw), 690 (w), 712 (vw), 749 (w), 757 (m), 772 (vs), 794 (m), 805 (w), 822 (w), 869 (m), 886 (w), 934 (w), 1003 (w), 1039 (m), 1057 (w), 1096 (w), 1104 (w), 1142 (vw), 1158 (vw), 1189 (w), 1203 (w), 1238 (s), 1255 (w), 1312 (m), 1357 (w), 1376 (m), 1387 (m), 1431 (s), 1463 (w), 1527 (vs), 1588 (vw), 1617 (vw), 2865 (w), 2955 (m) cm^{-1}. Elemental analysis (calcd.) [%]: C: 75.94 (76.72), H: 8.88 (9.01), N: 6.06 (5.96).

L5H: A mixture of 9 g P_4O_{10} (1 equiv., 63.4 mmol) and 40 mL hexamethyldisiloxane (3 equiv., 187.2 mmol) in 40 mL CH_2Cl_2 was refluxed at 65 °C for 45 min. After cooling down to room temperature the solvent was removed in vacuo. The resulting viscous polyphosphoric acid trimethylsilyl ester (PPSE) was heated to 160 °C and reacted with 1.245 g terephthalic acid (7.5 mmol) and 4.8 mL mesitylamine (30 mmol), in quick succession. The fuming mixture was stirred overnight at 160 °C. The resulting viscous yellow body was poured hot into 250 mL of 1 M $NaOH_{aq}$. After cooling to room temperature 200 mL of CH_2Cl_2 were added and vigorously stirred for several hours. After separation of the organic layer, the aqueous was extracted three times with 50 mL of CH_2Cl_2 each. The combined organic phase was dried with $MgSO_4$, filtered and evacuated to dryness. The residue was refluxed in hexane, filtered off and dried again. After crystallization from 50 mL of boiling CH_2Cl_2 and washing with hexane, **L5H** can be obtained as a colorless solid, pure enough for further reactions (3.3 g, 5.2 mmol, 69 %). **L5H** dissolves in C_6D_6 forming aggregates. The measured NMR spectra show a variety of very broad signals that could not be fully assigned using correlation methods. The signals are mentioned for the identification of the product. ^{1}H NMR (400.1 MHz, 298 K, C_6D_6): δ = 1.80, 1.83, 1.98, 2.02, 2.16, 2.27, 2.30 (multiple overlapping broad signals, 48 H, mesityl CH_3), 4.62, 5.00, 5.33 (3s, 2 H, NH), 6.43, 6.50, 6.71, 6.84, 6.94, 7.11 7.48, 7.50, 7.55 (multiple broad signals, 12 H, mesityl and phenyl CH) ppm. ^{13}C NMR (100.6 MHz, 298 K, C_6D_6): δ = 18.3, 18.9, 20.9, 21.0 (4s, 12 C, mesityl CH_3), 126.9, 129.0, 129.4, 129.7, 131.7, 131.9, 134.9, 135.3, 135.8, 137.2, 144.4, 144.5, 152.8, 152.9 (multiple singlets, aromatic C) ppm. IR (ATR, $\tilde{\nu}$): $\tilde{\nu}$ = 425 (w), 471 (m), 507 (m), 563 (w), 574 (vw), 616 (w), 640 (w), 664 (w), 696 (m), 753 (vw), 791 (w), 849 (vs), 885 (m), 935 (vw), 960 (vw), 1011 (w), 1033 (w), 1113 (w), 1149 (w), 1213 (s), 1298 (w), 1348 (vs), 1401 (w), 1474 (s), 1514 (w), 1559 (w), 1604 (vs), 1620 (vs), 2731 (vw), 2854 (vw), 2915 (w), 2942 (vw), 2996 (vw), 3358 (vw) cm^{-1}. Elemental analysis (calcd.) [%]: C: 82.82 (83.24), H: 7.49 (7.94), N: 8.78 (8.82).

L5Na: 400 mg **L5H** (1 equiv., 0.63 mmol) was added to 243 mg Na[$N(SiMe_3)_2$] (2.1 equiv., 1.32 mmol) and stirred overnight in 10 mL of THF. The resulting yellow solution was reduced to ca. 7 mL and filtered into a thin Schlenk tube, using a syringe filter. The product can be crystallized by layering with 20 mL of hexane. The colorless crystals were washed with 5 mL of hexane and dried in vacuo (398 mg, 0.48 mmol, 77 %). ^{1}H NMR (400.1 MHz, 298 K, [D_8]THF): δ = 1.82 (s, 24 H, *ortho* CH_3), 2.04 (s, 12 H, *para* CH_3), 6.18 (br., 2 H, phenyl CH), 6.39 (s, 8 H, mesityl CH), 6.69 (m, 2 H, Phenyl CH) ppm. ^{13}C NMR (100.6 MHz, 298 K, [D_8]THF): δ = 20.0 (s, 8 C, *ortho* CH_3), 21.2 (s, 4 C, *para* CH_3), 126.1 (s, 4 C, mesityl *ipso* C), 127.3 (s, C_{quart}), 128.5 (s, 8 C, mesityl CH), 130.8 (s, 4 C, *para* CCH_3), 152.1 (s, 8 C, *ortho* CCH_3) ppm. The remaining carbon signals could not be de-

© 0000 Wiley-VCH Verlag GmbH & Co. KGaA, Weinheim

tected. IR (ATR, $\tilde{\nu}$): $\tilde{\nu}$ = 500.1 (w), 522 (m), 581 (w), 626 (vw), 657 (w), 683 (w), 751 (w), 780 (vw), 845 (s), 854 (s), 886 (m), 903 (w), 920 (w), 958 (vw), 1003 (w), 1047 (s), 1120 (w), 1145 (w), 1208 (s), 1253 (w), 1298 (w), 1342 (w), 1369 (m), 1456 (vs), 1563 (vw), 2854 (vw), 2885 (vw), 2914 (vw), 2958 (vw), 2988 (vw) cm^{-1}. Elemental analysis (calcd.) [%]: C: 75.78 (75.88), H: 7.76 (7.84), N: 6.74 (6.81).

L6H: A mixture of 9 g P_4O_{10} (1 equiv., 63.4 mmol) and 40 mL hexamethyldisiloxane (3 equiv., 187.2 mmol) in 40 mL CH_2Cl_2 was refluxed at 65 °C for 45 min. After cooling down to room temperature the solvent was removed in vacuo. The resulting viscous polyphosphoric acid trimethylsilyl ester (PPSE) was heated to 160 °C and reacted with 1.245 g isophthalic acid (7.5 mmol) and 4.8 mL mesitylamine (30 mmol), in quick succession. The fuming mixture was stirred overnight at 160 °C. The resulting viscous yellow body was poured hot into 250 mL of 1 M $NaOH_{aq}$. After cooling to room temperature 200 mL of CH_2Cl_2 were added and vigorously stirred for several hours. After separation of the organic layer, the aqueous was extracted three times with 50 mL of CH_2Cl_2 each. The combined organic phase was dried with $MgSO_4$, filtered and evacuated to dryness. To remove residual mesitylamine the body was dried for 6 d at 70 °C in vacuo. It was then refluxed in 10 mL Et_2O, let cool down to room temperature and filtered off. This procedure was repeated with another 10 mL of Et_2O and two times with 10 mL of hexane. After drying in vacuo the white **L6H** contains only marginal amounts of mesitylamine and can is pure enough for further reactions (2.4 g, 3.8 mmol, 50 %). **L6H** dissolves in C_6D_6 forming aggregates. Measured NMR spectra show a variety of very broad signals that could not be fully assigned using correlation methods. The signals are mentioned for the identification of the product. ^{1}H NMR (400.1 MHz, 298 K, C_6D_6): δ = 1.82, 1.91, 1.92, 2.05, 2.08, 2.13, 2.18, 2.21, 2.29, 2.32, 2.37, 2.41 (overlapping broad signals, 48 H, mesityl CH_3), 4.86, 5.36, 5.38 (3s, 2 H, NH), 6.50, 6.52, 6.69, 6.72, 6.74, 6.81, 6.98, 7.37, 7.42, 7.58, 7.61, 7.72, 7.85 (broad signals, 12 H, mesityl and phenyl CH) ppm. ^{13}C NMR (100.6 MHz, 298 K, C_6D_6): δ = 14.4, 18.3, 19.0, 19.1, 20.7, 20.9, 21.0, 23.1 (8s, 12 C, mesityl CH_3), 129.1, 129.4, 129.7, 131.7, 131.9, 134.8, 135.1, 135.4, 135.6, 136.1, 136.5, 144.4, 144.6, 152.5, 152.8 (multiple singlets, aromatic C) ppm. IR (ATR, $\tilde{\nu}$): $\tilde{\nu}$ = 410 (vw), 418 (vw), 425 (vw), 435 (vw), 484 (w), 509 (w), 557 (m), 573 (vw), 600 (vw), 638 (w), 705 (s), 749 (vw), 782 (m), 813 (w), 851 (vs), 886 (w), 935 (vw), 1010 (w), 1032 (w), 1094 (w), 1112 (w), 1149 (w), 1214 (s), 1246 (m), 1281 (w), 1346 (m), 1372 (m), 1433 (s), 1473 (vs), 1576 (s), 1596 (s), 1623 (vs), 2728 (vw), 2854 (vw), 2914 (w), 3222 (vw), 3344 (vw), 3380 (vw) cm^{-1}. Elemental analysis (calcd.) [%]: C: 82.30 (83.24), H: 7.73 (7.94), N: 8.50 (8.82).

L6Na: 200 mg **L6H** (1 equiv., 0.32 mmol) was added to 122 mg $Na[N(SiMe_3)_2]$ (2.1 equiv., 0.63 mmol) and stirred overnight in 5.5 mL of DME. The resulting yellow solution was filtered into a thin Schlenk tube, using a syringe filter. The product was crystallized by layering with 10 mL of hexane. The colorless crystals were washed with 5 mL of hexane and dried in vacuo (200 mg, 0.23 mmol, 72 %). ^{1}H NMR (400.1 MHz, 298 K, [D_6]DMSO): δ = 1.99 (s, 24 H, *ortho* CH_3), 2.06 (s, 12 H, *para* CH_3), 3.24 (s, 12 H, DME CH_3), 3.43 (s, 8 H, DME CH_2), 6.46 (s, 8 H, mesityl CH, 1 H, phenyl CH), 6.80 (br., 2 H, phenyl CH), 7.90 (s, 1 H, phenyl CH) ppm. ^{13}C NMR (100.6 MHz, 298 K, [D_6]DMSO): δ = 19.5 (s, 8 C, *ortho* CH_3), 20.6 (s, 4 C, *para* CH_3), 58.0 (s, 4 C, DME CH_3), 71.1 (s, 8 H, DME CH_2), 98.5 (s, C_{quart}), 127.2 (s, 8 C, mesityl CH), 129.0 (s, 2 C, phenyl CH), 153.6 (s, 8 C, *ortho* CCH_3) ppm. The remaining ^{13}C NMR signals could not be detected. IR (ATR, $\tilde{\nu}$): $\tilde{\nu}$ = 408 (vw), 419 (vw), 423 (vw), 439 (vw), 471 (vw), 492 (vw), 505 (vw), 533 (vw), 559 (m), 573 (vw), 643 (vw), 715 (m), 733 (w), 749 (vw), 787 (m), 814 (w), 827 (w), 849 (vs), 899 (w), 914 (w), 962 (vw), 1006 (w), 1030 (w), 1077 (vs), 1084 (vs), 1126 (m), 1150 (w), 1215 (vs), 1245 (w), 1293 (w), 1373 (s), 1426 (s), 1464 (vs), 1501 (vs), 1598 (vw), 1628 (vw), 2905 (w) cm^{-1}. Elemental analysis (calcd.) [%]: C: 72.53 (72.70), H: 7.61 (7.98), N: 6.86 (6.52).

L7a: A solution of 4.3 mL (0.25 equiv., 0.05 mol) oxalyl chloride in 30 mL toluene was added dropwise to a solution of 28.1 mL mesitylamine (1 equiv., 0.20 mol) in 100 mL toluene. The reaction was stirred for 6 h at 70 °C. After cooling down to room temperature the white solid was filtered off, washed with 0.5 l toluene and reduced to dryness. The solid was washed in multiple portions with 1 l water each. The colorless product was dried in vacuo for 24 h at 70 °C and brought into inert atmosphere. Yield: 14.3 g (0.044 mmol, 88 %). ^{1}H NMR (400.1 MHz, 298 K, C_6D_6): δ = 2.08 (s, 6 H, *para* CH_3), 2.09 (s, 12 H, *ortho* CH_3), 6.68 (s, 4 H, mesityl CH), 8.59 (br., 2 H, NH) ppm. ^{13}C NMR (100.6 MHz, 298 K, C_6D_6): δ = 18.4 (s, 4 C, *ortho* CH_3), 20.9 (s, 2 C, *para* CH_3), 129.2 (s, 4 C, mesityl CH), 130.8 (s, 2 C, mesityl C_{quart}), 134.9 (s, 4 C, *ortho* CCH_3), 137.1 (s, 2 C, mesityl C_{quart}), 158.6 (s, 2 C, OCN) ppm. IR (ATR, $\tilde{\nu}$): $\tilde{\nu}$ = 468 (vs), 490 (s), 518 (vs), 555 (w), 596 631 (m), 704 (s), 731 (m), 857 (s), 880 (w), 940 (vw), 1015 (vw), 1038 (vw), 1175 (vw), 1226 (w), 1253 (vw), 1284 (vw), 1311 (vw), 1376 (w), 1440 (s), 1467 (s), 1490 (s), 1608 (vw), 1712 (vw), 2863 (vw), 2919 (vw), 2960 (vw), 3343 (vw) cm^{-1}. Elemental analysis (calcd.) [%]: C: 73.82 (74.05), H: 7.00 (7.46), N: 8.55 (8.63).

L7b: 28.5 g PCl_5 (3.1 equiv., 0.137 mol) were added to a suspension of 14.27 g L**7a** (1 equiv., 0.044 mol) in 60 mL of toluene and the reaction mixture was heated to reflux for 6 h. The yellow solution was reduced to ca. 1/3 of its volume and stored overnight at –35 °C. The obtained yellow crystals were filtered off and dried in vacuo at 50 °C using a trap-to-trap arrangement. Yield: 14.3 g (0.039 mol, 90 %). ^{1}H NMR (400.1 MHz, 298 K, C_6D_6): δ = 2.10 (s, 12 H, *ortho* CH_3), 2.12 (s, 6 H, *para* CH_3), 6.75 (s, 4 H, *meta* CH) ppm. ^{13}C NMR (100.6 MHz, 298 K, C_6D_6): δ = 17.8 (s, 4 C, *ortho* CH_3), 20.8 (s, 2 C, *para* CH_3), 125.5 (s, 2 C, *ipso* C), 129.2 (s, 4 C, *meta* CH), 134.8 (s, 2 C, *para* CCH_3), 138.9 (s, 2 C, ClCN), 142.9 (s, 4 C, *ortho* CCH_3) ppm. IR (ATR, $\tilde{\nu}$): $\tilde{\nu}$ = 458 (vw), 533 (vw), 575 (vw), 612 (vw), 697 (vw), 728 (vw), 810 (vw), 853 (s), 885 (vs), 952 (w), 1023 (vs), 1035 (vs), 1139 (vw), 1200 (vw), 1252 (vw), 1305 (vw), 1374 (m), 1381 (m), 1442 (vw), 1466 (vw), 1609 (vw), 1625 (vw), 1669 (w), 1732 (m), 2857 (vw), 2917 (vw) cm^{-1}. Elemental analysis (calcd.) [%]: C: 65.62 (66.49), H: 5.67 (6.14), N: 7.56 (7.75).

L7H: 15.6 mL mesitylamine (7.9 equiv., 110.9 mmol) were added to a suspension of 5.00 g L**7b** (1 equiv., 13.9 mmol) in 50 mL toluene. The reaction mixture was stirred at 120 °C for 4 h before the oil bath was removed and stirring continued overnight. The solvent was removed in vacuo. In order to remove unconsumed mesitylamine drying was continued for 5 d at 70 °C using a trap-to-trap arrangement. The obtained solid was treated with 20 mL of hexane, filtered off and washed with further 40 mL of hexane. To remove the reaction byproduct mesitylammonium hydrochloride, the solid was than suspended in 400 mL of toluene, parted in halves and extracted three times with 300 mL H_2O, each. The organic layers were combined and the solvent was removed. The resulting solid was again washed two times with 60 mL hexane and evacuated to dryness. The tedious drying and washing steps serve the purpose of removing residual mesitylamine. Yield: 4.80 g (8.60 mmol, 62 %). ^{1}H NMR (400.1 MHz, 298 K, C_6D_6): δ = 2.09 (s, 12 H, *para* CH_3), 2.19 (s, 24 H, *ortho* CH_3), 6.57 (s, 8 H, mesityl CH), 8.89 (br., 2 H, NH) ppm. ^{13}C NMR (100.6 MHz, 298 K, C_6D_6): δ = 19.1 (s, 8 C, *ortho* CH_3), 20.9 (s, 4 C, *para* CH_3), 128.2 (s, 8 C, mesityl CH) ppm. The other ^{13}C NMR resonances could not be detected. IR (ATR, $\tilde{\nu}$): $\tilde{\nu}$ = 433 (vw), 465 (m), 495 (m), 523 (m), 552 (m), 575 (vw), 590 (vw), 624 (vw), 641 (vw), 653 (vw), 675 (v), 695 (vw), 715 (vw), 726 (vw), 744 (vw), 784 (m), 822 (vw), 850 (s), 879 (m), 935 (vw), 957 (vw), 1012 (w), 1031 (w), 1140 (w), 1195 (w), 1213 (s), 1260 (vs), 1311 (w), 1369 (w), 1408

© 0000 Wiley-VCH Verlag GmbH & Co. KGaA, Weinheim

(m), 1431 (w), 1473 (s), 1603 (m), 1632 (vs), 2729 (vw), 2853 (vw), 2914 (vw), 2943 (vw), 2995 (vw) cm^{-1}. Elemental analysis (calcd.) [%]: C: 81.69 (81.68), H: 7.81 (8.30), N: 9.79 (10.03).

Rhodium(I) Complexes

1: 200 mg of **L1Li** (2 equiv., 0.536 mmol) and 132 mg $[Rh(cod)Cl]_2$ (1 equiv., 0.267 mmol) were added to a Schlenk tube dissolved in 15 mL of THF and stirred for two days. The mixture was evacuated to dryness and the residual solid extracted with 8 mL of toluene. For the separation of the LiCl the yellow mixture was filtered through a syringe filter within a glovebox and reduced to dryness. The resulting yellow solid was recrystallized from 5 mL of hexane within a closed flask at 100 °C. Yield: 148 mg (0.293 mmol, 55 %). ^{1}H NMR (400.1 MHz, 298 K, C_6D_6): δ = 1.06 (s, 3 H, N_2CCH_3), 1.51 (m, 4 H, COD CH_2), 2.18 (s, 6H *para* CH_3), 2.27 (m, 4 H, COD CH_2), 2.52 (s, 12 H, *ortho* CH_3), 3.76 (s, 4 H, COD CH), 6.84 (m, 4 H, mesityl CH) ppm. ^{13}C NMR (100.6 MHz, 298 K, C_6D_6): δ = 15.2 (d, JC_{Rh} = 1.7 Hz, 1 C, N_2CCH_3), 18.9 (s, 4 C, *ortho* CH_3), 21.0 (s, 2 C, *para* CH_3), 31.4 (s, 4 C, COD CH_2), 77.8 (d, J_{CRh} = 12.8 Hz, 4 C, COD CH), 129.0 (s, 4 C, mesityl CH), 133.1 (s, 2 C, ipso C), 133.6 (s, 4 C, *ortho* CCH_3), 141.6 (s, 2 C, *para* CCH_3), 179.1 (d, J_{CRh} = 5.4 Hz, 1 C, N_2C) ppm. IR (ATR, $\tilde{\nu}$): $\tilde{\nu}$ = 466 (m), 480 (m), 501 (w), 517 (w), 535 (w), 560 (m), 633 (vw), 692 (vw), 721 (vw), 745 (vw), 768 (vw), 784 (vw), 811 (vw), 857 (vs), 884 (vw), 948 (w), 981 (m), 1033 (w), 1150 (s), 1222 (vs), 1260 (vs), 1301 (w), 1356 (w), 1374 (w), 1428 (m), 1475 (s), 2728 (vw), 2827 (vw), 2872 (vw), 2916 (vw), 2936 (vw), 2964 (vw), 2991 (vw) cm^{-1}. Elemental analysis (calcd.) [%]: C: 66.74 (66.66), H: 7.20 (7.39), N: 5.53 (5.55).

2: 200 mg **L2Na** (1.0 equiv., 0.439 mmol) were added to 107 mg $[Rh(cod)Cl]_2$ (0.5 equiv., 0.217 mmol) and dissolved in 15 mL of THF. The mixture was stirred for 12 h and reduced to dryness. The residue was extracted with 8 mL of toluene and filtered through a syringe filter within a glovebox. The solution was reduced to half of its volume and stored at –35 °C. After two days the resulting crystals were separated using a syringe, washed with a small amount of cold hexane and dried in vacuo. Yield: 90 mg (0.153 mmol, 35 %). ^{1}H NMR (400.1 MHz, 298 K, C_6D_6): δ = 1.21 (s, 3 H, N_2CCH_3), 1.31 (d, ^3J = 6.9 Hz, 12 H, Dipp CH_3), 1.48 (d, ^3J = 6.9 Hz, 12 H, Dipp CH_3), 1.52 (m, 4 H, COD CH_2), 2.30 (m, 4 H, COD CH_2), 3.78 (br., 4 H, COD CH), 4.04 [sept, ^3J = 6.9 Hz, $CH(CH_3)_2$], 7.11 (s, 6 H, Dipp CH) ppm. ^{13}C NMR (100.6 MHz 298 K, C_6D_6): δ = 16.3 (d, J_{CRh} = 1.7 Hz, 1 C, N_2CCH_3), 24.3 (s, 4 C, Dipp CH_3), 24.7 (s, 4 C, Dipp CH_3), 28.3 [s, 4 C, Dipp $CH(CH_3)_2$], 31.1 (s, 4 C, COD CH_2), 78.2 (d, J_{CRh} = 12.8 Hz, 4 C, Dipp CH), 123.5 (s, 4 C, Dipp CH), 125.3 (s, 2 C, Dipp CH), 141.0 (s, 2 C, Dipp *ipso* C), 180.2 (d, J_{CRh} = 5.3 Hz, N_2C) ppm. IR (ATR, $\tilde{\nu}$): $\tilde{\nu}$ = 413 (w), 442 (m), 482 (w), 491 (w), 521 (w), 540 (m), 587 (vw), 685 (w), 719 (w), 747 (vs), 765 (s), 789 (vs), 802 (w), 816 (vw), 848 (w), 868 (w), 933 (w), 954 (w), 978 (w), 991 (w), 1045 (vw), 1057 (w), 1077 (vw), 1098 (w), 1153 (w), 1175 (w), 1193 (w), 1218 (m), 1245 (m), 1263 (vs), 1320 (s), 1340 (w), 1362 (vs), 1381 (m), 1430 (vs), 1443 (s), 1460 (vs), 1481 (s), 2830 (w), 2867 (w), 2919 (w), 2956 (m), 2999 (vw), 3056 (vw) cm^{-1}. Elemental analysis (calcd.) [%]: C: 69.62 (69.37), H: 8.02 (8.39), N: 4.73 (4.76).

3: A solution of $[Rh(cod)Cl]_2$ (25.0 mg, 0.05 mmol) in toluene (3 mL) was added dropwise to a solution of **L3Na** (49.0 mg, 0.10 mmol) at –30 °C and then stirred at room temperature for 1 h. After filtration, the red solution was kept at –30 °C, whereupon **3** was obtained as yellow crystals. Yield: 22 mg (37 %). ^{1}H NMR (300 MHz, 298 K, C_6D_6): δ = 1.47 [d, $^3J_{HH}$ = 6.86 Hz, 12 H, $CH(CH_3)_2$], 1.50 [d, $^3J_{HH}$ = 6.86 Hz, 12 H, $CH(CH_3)_2$], 1.50 (m, 4 H, COD-CH_2), 1.68 (s, 1 H, C≡C*H*) 2.25 (br., 4 H, COD-CH_2), 3.82 (br., 4 H, COD-C*H*), 4.09 [sept, $^3J_{HH}$ = 6.89 Hz, 4 H, $CH(CH_3)_2$], 6.99–7.12 ppm (m, 6 H, Ar-*H*). ^{13}C NMR (75 MHz, 298 K, C_6D_6): δ = 24.7 [$CH(CH_3)_2$], 24.9 [$CH(CH_3)_2$], 28.8 [$CH(CH_3)_2$] 30.9 (COD-CH_2), 79.0 (d, $^1J_{RhC}$ = 13.02 Hz; COD-CH), 82.6 (C≡CH), 123.1 (*p*-Ar-*C*), 125.5 (*m*-Ar-*C*), 140.7 (*o*-Ar-C_{ipso}), 144.4 ppm (Ar-C_{ipso}-N). IR (ATR, $\tilde{\nu}$): $\tilde{\nu}$ = 429 (w), 783 (s), 1097 (w), 1253 (w), 1322 (w), 1471 (vs), 2103 (vw), 2865 (vw), 2957 (w), 3255 (vw) cm^{-1}. EI/MS: *m/z* (%) = 598.31 (24.46) $[M]^+$. m.p. 175 °C (dec); No satisfactory elemental analysis could be obtained, due to the limited stability of **3**.

4: A solution of 100 mg **L4Na** (1 equiv., 0.107 mmol) in 8 mL THF was added dropwise to a solution of 53 mg $[Rh(cod)Cl]_2$ (1 equiv., 0.107 mmol) in 12 mL THF in an ice bath. After stirring overnight, the reddish-brown suspension was evacuated to dryness and extracted with 5 mL toluene. The mixture was filtered into a thin Schlenk tube and reduced to approximately 3 mL. The solution was layered with 9 mL Et_2O and stored in the fridge (–35 °C) for several months. **6** slowly precipitates in form of red crystals containing one molecule Et_2O per formula unit. The crystals were washed with Et_2O and dried in vacuo. Yield: 38 mg (0.0324 mmol, 30 %). ^{1}H NMR (400.1 MHz, 298 K, C_6D_6): δ = 1.03 (d, ^3J = 6.9 Hz, 24 H, Dipp CH_3), 1.33 (m, 8 H, COD CH_2), 1.52 (d, ^3J = 6.9 Hz, 24 H, Dipp CH_3), 2.09 (m, 8 H, COD CH_2), 3.42 (br., 8 H, COD CH), 3.67 [sept, ^3J = 6.8 Hz, 8 H, Dipp $HC(CH_3)_2$], 7.01 (m, 12 H, Dipp Ar-CH) ppm. ^{13}C NMR (100.6 MHz, 298 K, C_6D_6): δ = 23.4 (s, 8 C, CH_3), 25.3 (s, 8 C, Dipp CH_3), 28.9 [s, 8 C, Dipp $CH(CH_3)_2$], 30.6 (s, 8 C, COD CH_2), 80.0 (d, $^1J_{CRh}$ = 12.7 Hz, COD CH), 81.6 (d, J_{CRh} = 3.0 Hz, 2 C, alkene CC), 123.3 (s, 8 C, meta CH), 125.3 (s, 4 C, para CH), 140.5 (s, 4 C, ipso C), 143.4 (s, 8 C, CCH_3), 159.0 (d, *J*CRh = 5.6 Hz, CN_2) ppm. IR (ATR, $\tilde{\nu}$): $\tilde{\nu}$ = 401 (m), 423 (m), 445 (m), 482 (w), 529 (w), 581 (vw), 662 (w), 689 (vw), 746 (s), 791 (s), 805 (w), 817 (vw), 864 (w), 879 (w), 937 (vw), 955 (w), 1000 (w), 1042 (vw), 1060 (vw), 1075 (vw), 1097 (w), 1112 (w), 1159 (vw), 1178 (w), 1222 (m), 1264 (m), 1324 (m), 1361 (m), 1381 (w), 1420 (m), 1464 (vs), 2831 (vw), 2868 (w), 2927 (w), 2956 (w), 3057 (vw) cm^{-1}. Elemental analysis (calcd.) [%]: C: 69.54 (69.73), H: 7.52 (7.92), N: 4.72 (4.78).

5: A mixture of 200 mg **L5Na** (1 equiv., 0.243 mmol) and 120 mg $[Rh(cod)Cl]_2$ (1 equiv., 0.243 mmol) in 20 mL of THF was stirred in an ice bath. The compounds slowly dissolve, whilst an orange solid precipitates. After stirring overnight, the mixture was dried in vacuo and 25 mL of toluene were added. The red suspension was filtered through a syringe filter into a thin Schlenk tube and the solvent was reduced, until the formation of precipitate. The mixture was heated, until everything was fully dissolved and layered with 40 mL of hexane. After diffusion the obtained orange red crystals were filtered off, washed with hexane and dried in vacuo (189 mg, 0.164 mmol, 68 %). ^{1}H NMR (400.1 MHz, 298 K, C_6D_6): δ = 1.44 (m, 8 H, COD CH_2), 2.08 (s, 12 H, *para* CH_3), 2.15 (br., 8 H, COD CH_2), 2.32 (s, 24 H, *ortho* CH_3), 3.74 (br., 8 H, COD CH), 6.61 (s, 8 H, mesityl CH), 6.84 (s, 4 H, phenyl CH) ppm. ^{13}C NMR (100.6 MHz, 298 K, C_6D_6): δ = 19.1 (s, 8 C, *ortho* CH_3), 21.0 (s, 4 C, *para* CH_3), 31.2 (s, 8 C, COD CH_2), 78.7 (d, J_{CRh} = 12.7 Hz, COD CH), 126.8 (s, 2 C, phenyl CCN_2), 128.7 (s, 4 C, phenyl $CHCCN_2$), 129.1 (s, 8 C, mesityl CH), 132.5 (s, 4 C, *para* CCH_3), 132.6 (s, 4 C, mesityl *ipso* C), 141.7 (s, 8 C, *ortho* CCH_3), 178.2 (d, J_{CRh} = 5.1 Hz, CN_2) ppm. IR (ATR, $\tilde{\nu}$): $\tilde{\nu}$ = 457 (vw), 482 (w), 499 (w), 542 (w), 575 (s), 646 (w), 671 (w), 741 (w), 782 (w), 814 (w), 846 (s), 885 (vw), 950 (w), 964 (m), 990 (w), 1005 (w), 1031 (w), 1076 (vw), 1117 (w), 1147 (w), 1173 (w), 1207 (s), 1268 (m), 1301 (w), 1326 (w), 1371 (m), 1385 (m), 1430 (s), 1475 (vs), 1568 (vw), 1719 (vw), 2726 (vw), 2831 (vw), 2876 (vw), 2914 (w), 3001 (vw) cm^{-1}. Elemental analysis (calcd.) [%]: C: 68.37 (68.30), H: 6.60 (6.88), N: 5.16 (5.31).

6: 150 mg **L6Na** (1 equiv., 0.175 mmol) and 86 mg $[Rh(cod)Cl]_2$ (1 equiv., 0.175 mmol) were weighed into a Schlenk tube and stirred in 10 mL of THF overnight. The orange reaction mixture was evacuated to dryness. The resulting reaction mixture was extracted with 10 mL of hot toluene and separated using a syringe filter. After

© 0000 Wiley-VCH Verlag GmbH & Co. KGaA, Weinheim

cooling down to room temperature, the solution was layered with 20 mL of hexane. After completion of the diffusion, the obtained crystals were filtered of, washed with cold hexane and dried in vacuo [Yield: 100.1 mg (0.095 mmol, 51 %)]. ^{1}H NMR (400.1 MHz, 298 K, C_6D_6): δ = 1.46 (m, 8 H, COD CH_2), 2.13 (s, 12 H, *para* CH_3), 2.20 (br., 8 H, COD CH_2), 2.36 (s, 24 H, *ortho* CH_3), 3.78 (s, 8 H, COD CH), 6.37 [m, 1 H, $N_2CC(CH)CH$], 6.69 [$_{pseudo}$t, J = 1.7, 0.48 Hz, 1 H, $N_2CC(CH)$], 6.74 (s, 8 H, mesityl CH), 6.87 [dd, J = 7.8, 1.7 Hz, 2 H, $N_2CC(CH)$] ppm. ^{13}C NMR (100.6 MHz, 298 K, C_6D_6): δ = 19.4 (s, 4 C, *para* CH_3), 21.1 (s, 8 C, *ortho* CH_3), 31.2 (s, 16 C, COD CH_2), 78.7 (d, J_{CRh} = 12.7 Hz, 8 C, COD CH), 125.9 [s, 1 C, $N_2CC(CH)$], 127.0 [s, 1 C, $N_2CC(CH)CH$], 128.7 [s, 2 C, $N_2CC(CH)$], 129.1 (s, 8 C, mesityl CH), 132.6 (s, 4 C, para CCH_3), 132.9 (s, 2 C, N_2CC), 134.0 (d, J_{CRh} = 5.3 Hz, mesityl *ipso* C), 141.6 (s, 8 C, *ortho* CCH_3), 178.7 (d, J_{CRh} = 5.3 Hz, 2 C, N_2C) ppm. IR (ATR, $\tilde{\nu}$): $\tilde{\nu}$ = 483 (w), 493 (w), 499 (w), 515 (w), 575 (m), 587 (m), 594 (w), 646 (w), 677 (w), 698 (w), 717 (m), 752 (m), 768 (w), 782 (w), 793 (w), 815 (w), 830 (w), 852 (w), 894 (vs), 937 (w), 949 (w), 974 (w), 991 (w), 1005 (w), 1029 (w), 1149 (vw), 1163 (w), 1175 (w), 1212 (w), 1258 (s), 1275 (s), 1300 (w), 1325 (w), 1373 (w), 1390 (m), 1429 (m), 1452 (vs), 1475 (vs), 1582 (vs), 1602 (vw), 1723 (vw), 2728 (vw), 2828 (vw), 2873 (w), 2913 (w), 2938 (w), 2957 (w), 2999 (vw) cm^{-1}. Elemental analysis (calcd.) [%]: C: 68.74 (68.30), H: 6.61 (6.88), N: 5.41 (5.31).

7: 113 mg **L7H** (1 equiv., 0.202 mmol), 100 mg $[Rh(COD)Cl]_2$ (1 equiv., 0.202 mmol) and 75 mg $Na[N(SiMe_3)_2]$ 1.02 equiv., 0.409 mmol were placed in a Schlenk tube, cooled in an ice bath and mixed with 10 mL toluene. After stirring overnight, the brownish suspension was evacuated to dryness. The obtained solid was extracted with 10 mL dichloromethane, using an ultrasonic bath, filtered off and washed with additional 6 mL dichloromethane and two times with H_2O. After drying in vacuo the yellow **7** was obtained. Yield: 121 mg (124 mmol, 61 %). ^{1}H NMR (400.1 MHz, 298 K, C_6D_6): δ = 1.38 (m, 8 H, COD CH_2), 2.06 (s, 12 H, *para* CH_3), 2.11 (m, 8 H, COD CH_2), 2.59 (s, 24 H, *ortho* CH_3), 2.84 (br., 8 H, COD CH), 6.45 (br., 8 H, mesityl CH) ppm. ^{13}C NMR (100.6 MHz, 298 K, C_6D_6): δ = 20.8 (s, 4 C, *para* CH_3), 21.0 (s, 8 C, *ortho* CH_3), 30.8 (s, 8 C, COD CH_2), 81.2 (d, J_{CRh} = 12.7 Hz, 8 C, COD CH), 128.7 (s, 8 C, *meta* CH), 132.0 (s, 4 C, C_{quart}), 132.1 (s, 4 C, *ortho* CCH_3), 143.2 (s, 4 C, C_{quart}) ppm. The missing signal for the center N_2CCN_2 carbon atoms could not be detected. IR (ATR, $\tilde{\nu}$): $\tilde{\nu}$ = 462 (vw), 483 (vw), 514 (vw), 532 (vw), 597 (m), 632 (vw), 694 (vw), 726 (w), 783 (s), 825 (w), 850 (vw), 864 (w), 890 (vw), 944 (w), 966 (vw), 996 (w), 1010 (w), 1031 (vw), 1079 (vw), 1110 (w), 1150 (vw), 1177 (vw), 1215 (vw), 1227 (vw), 1242 (vw), 1299 (vw), 1339 (w), 1367 (w), 1431 (vw), 1446 (w), 1475 (m), 1489 (vs), 1514 (vs), 1596 (vw), 2821 (vw), 2872 (w), 2914 (vw), 2943 (vw) cm^{-1}. Elemental analysis (calcd.) [%]: C: 66.21 (66.25), H: 6.63 (7.00), N: 5.67 (5.72).

8: 120 mg **7** (0.123 mmol) were suspended in 20 mL toluene. The mixture was degassed by three freeze-pump-thaw cycles and brought under an atmosphere of 2 bar CO. During stirring for 2 h at 70 °C the barely soluble **7** completely dissolves. After drying in vacuo the yellow **8** was obtained. Yield: 102 mg (0.117 mmol, 95 %). ^{1}H NMR (400.1 MHz, 298 K, C_6D_6): δ = 2.02 (s, 12 H, *para* CH_3), 2.52 (s, 24 H, *ortho* CH_3), 6.43 (m, 8 H, *meta* CH) ppm. ^{13}C NMR (100.6 MHz, 298 K, C_6D_6): δ = 20.3 (s, 8 C, *ortho* CH_3), 20.8 (s, 4 C, *para* CH_3), 128.6 (s, 8 C, *meta* CH), 130.6 (s, 8 C, *ortho* CCH_3), 133.8 (s, 4 C, *para* CCH_3), 146.7 (s, 4 C, *ipso* C), 171.0 (t, J_{CRh} = 1.2 Hz, 2 C, CN_2), 184.9 (d, $^1J_{CRh}$ = 67.3 Hz, 4 C, CO) ppm. IR (ATR, $\tilde{\nu}$): $\tilde{\nu}$ = 406 (vw), 427 (vw), 453 (w), 507 (w), 521 (m), 537 (w), 617 (w), 695 (vw), 727 (vw), 835 (vw), 855 (m), 958 (w), 1010 (vw), 1028 (vw), 1110 (w), 1179 (vw), 1209 (vw), 1260 (vw), 1299 (vw), 1349 (w), 1371 (w), 1439 (w), 1473 (m), 1548 (s), 1610 (vw), 1971 (w), 2004 (vs) (CO), 2060 (vs) (CO), 2858 (vw), 2921 (vw), 2952 (vw) cm^{-1}. Elemental analysis (calcd.) [%]: C: 57.78 (57.68), H: 4.83 (5.07), N: 6.34 (6.41).

Crystal Structure Determinations

Crystal data collection and processing parameters are given below. In order to avoid quality degradation, the single crystals were mounted in perfluoropolyalkyl ether oil on top of an open Mark tube and then brought into the cold nitrogen stream of a low-temperature device (Oxford Cryosystems Cryostream unit) so that the oil solidified. Diffraction data were measured using a Stoe IPDS II diffractometer and graphite-monochromated Mo-K_α (0.71073 Å) radiation. The structures were solved by dual-space direct methods with SHELXT,[40] followed by full-matrix least-squares refinement using SHELXL-2014/7.[40] All non-hydrogen atoms were refined anisotropically. The contribution of the hydrogen atoms, in their calculated positions, was included in the refinement using a riding model.

CCDC 1830468 (for **L3Na**), 1830469 (for **L4Na**), 1830470 (for **L5H**), 1830471 (for **L5Na**), 1830472 (for **1**), 1830473 (for **2**), 1830474 (for **3**), 1830475 (for **4**), 1830476 (for **5**), 1830477 (for **6**), 1830478 (for **7**), and 1830479 (for **8**) contain the supplementary crystallographic data for this paper. These data can be obtained free of charge from The Cambridge Crystallographic Data Centre.

L3Na: $C_{35}H_{55}N_2Na_1O_4$, 590.80 g mol^{-1}, monoclinic, $P2_1/n$,[41] a = 1069.6(2), b = 1909.9(4), c = 1763.2(4) pm, β = 105.266(6)°, V = 3517.5(12) × 10^6 pm^3, T = 200(2) K, Z = 2, μ(Mo-K_α) = 0.082 mm^{-1}, $D_{calcd.}$ = 1.116 g cm^{-3}; crystal dimensions 0.2 × 0.2 × 0.2 mm^3, 26813 reflections, 25395 unique data, R_{int} = 0.0538; 395 parameters, wR_2 (all data) = 0.1411, S = 1.107 (all data), R_1 = 0.0525 [5429 data with $I > 2\sigma(I)$], max/min residual electron density: +0.29/–0.20 e 10^{-6} pm^{-3}.

L4Na: $C_{60}H_{84}N_4Na_2O_2$, orthorhombic, $P2_12_12_1$, a = 1616.0(3), b = 1788.0(4), c = 1968.9(4) pm, V = 5689(2) × 10^6 pm^3, T = 200(2) K, Z = 4, μ(Mo-K_α) = 0.079 mm^{-1}, $D_{calcd.}$ = 1.097 g cm^{-3}; crystal dimensions 1.0 × 1.0 × 1.0 mm^3, 88540 reflections, 12394 unique data, R_{int} = 0.0985; 630 parameters, wR_2 (all data) = 0.1592, S = 1.082 (all data), R_1 = 0.0527 [10868 data with $I > 2\sigma(I)$], max/min residual electron density: +0.29/–0.25 e 10^{-6} pm^{-3}.

L5H: $C_{46}H_{54}Cl_4N_4$, 804.73 g mol^{-1}, monoclinic, $C2/c$, a = 1781.1(4), b = 1557.1(3), c = 1581.8(3) pm, V = 4357.0(15) × 10^6 pm^3, T = 200(2) K, Z = 4, μ(Mo-K_α) = 0.308 mm^{-1}, $D_{calcd.}$ = 1.227 g cm^{-3}; crystal dimensions 0.4 × 0.3 × 0.2 mm^3, 38638 reflections, 5410 unique data, R_{int} = 0.0743; 250 parameters, wR_2 = 0.1701, S = 1.059 (all data), R_1 = 0.0553 [3922 data with $I > 2\sigma(I)$], max/min residual electron density: +0.33/–0.47 e 10^{-6} pm^{-3}.

L5Na: $C_{52}H_{60}N_4Na_2O_2$, tetragonal, $P4_2/nbc$, a = 1477.7(2), b = 1477.7(2), c = 2172.0(4) pm, V = 4742.8(16) × 10^6 pm^3, T = 200(2) K, Z = 4, μ(Mo-K_α) = 0.085 mm^{-1}, $D_{calcd.}$ = 1.147 g cm^{-3}; crystal dimensions 0.4 × 0.4 × 0.3 mm^3, 21241 reflections, 2337 unique data, R_{int} = 0.0653; 142 parameters, wR_2 (all data) = 0.2568, S = 0.965 (all data), R_1 = 0.0751 [1097 data with $I > 2\sigma(I)$], max/min residual electron density: +0.28/–0.29 e 10^{-6} pm^{-3}.

1: $C_{28}H_{37}N_2Rh_1$, 504.50 g mol^{-1}, orthorhombic, $Pbca$, a = 1461.2(3), b = 1409.4(3), c = 2429.2(5) pm, V = 5002.7(17) × 10^6 pm^3, T = 200(2) K, Z = 8, μ(Mo-K_α) = 0.700 mm^{-1}, $D_{calcd.}$ = 1.3396 g cm^{-3}; crystal dimensions 0.4 × 0.4 × 0.3 mm^3, 83909 reflections, 6040 unique data, R_{int} = 0.0659; 287 parameters, wR_2 = 0.1014, S = 1.054 (all data), R_1 = 0.0362 [5158 data with $I > 2\sigma(I)$], max/min residual electron density: +0.39/–0.84 e 10^{-6} pm^{-3}.

2: $C_{34}H_{49}N_2Rh_1$, 588.66 g mol^{-1}, monoclinic, $C2/c$, a = 1249.8(3), b = 1843.8(4), c = 1337.9(3) pm, β = 95.82(3)°, V = 3067.1(11) × 10^6 pm^3,

© 0000 Wiley-VCH Verlag GmbH & Co. KGaA, Weinheim

T = 200(2) K, Z = 4, μ(Mo-K_α) = 0.580 mm^{-1}, $D_{calcd.}$ = 1.275 g cm^{-3}; crystal dimensions 0.3 × 0.3 × 0.3 mm^3, 22843 reflections, 3358 unique data, R_{int} = 0.0703; 174 parameters, wR_2 (all data) = 0.0732, S = 1.070 (all data), R_1 = 0.0281 [3110 data with $I > 2\sigma(I)$], max/min residual electron density: +0.45/–0.57 e 10^{-6} pm^{-3}.

3: $C_{38.5}H_{51}N_2Rh$, triclinic, $P\bar{1}$, a = 1063.9(2), b = 1267.3(3), c = 1500.5(3) pm, α = 68.08(3)°, β = 81.44(3)°, γ = 68.80(3)°, V = 1749.6(6) × 10^6 pm^3, T = 200(2) K, Z = 2, μ(Mo-K_α) = 0.515 mm^{-1}, $D_{calcd.}$ = 1.224 g cm^{-3}; crystal dimensions 0.10 × 0.05 × 0.05 mm^3, 12197 reflections, 6093 unique data, R_{int} = 0.0902; 415 parameters, wR_2 (all data) = 0.1521, S = 0.981 (all data), R_1 = 0.0566 [4157 data with $I > 2\sigma(I)$], max/min residual electron density: +0.98/–0.88 e 10^{-6} pm^{-3}.

4: $C_{72}H_{102}N_4O_1Rh_2$, 1245.39 g mol^{-1}, triclinic, $P\bar{1}$, a = 1288.7(3), b = 1404.7(3), c = 1844.6(4) pm, α = 80.78(3)°, β = 79.32(3)°, γ = 86.68(3)°, V = 3237.6(12) × 10^6 pm^3, T = 200(2) K, Z = 2, μ(Mo-K_α) = 0.555 mm^{-1}, $D_{calcd.}$ = 1.278 g cm^{-3}; crystal dimensions 0.4 × 0.3 × 0.2 mm^3, 51997 reflections, 14130 unique data, R_{int} = 0.1155; 731 parameters, wR_2 = 0.1478, S = 1.087 (all data), R_1 = 0.0468 [10599 data with $I > 2\sigma(I)$], max/min residual electron density: +0.79/–1.12 e 10^{-6} pm^{-3}.

5: $C_{60}H_{72}N_4Rh_2$, 1055.03 g mol^{-1}, monoclinic, $P2_1/c$, a = 1320.8(3), b = 2656.9(5), c = 1597.3(3) pm, β = 114.42(3)°, V = 5104(2) × 10^6 pm^3, T = 200(2) K, Z = 4, μ(Mo-K_α) = 0.689 mm^{-1}, $D_{calcd.}$ = 1.373 g cm^{-3}; crystal dimensions 0.4 × 0.1 × 0.1 mm^3, 73322 reflections, 10039 unique data, R_{int} = 0.0989; 608 parameters, wR_2 = 0.1196, S = 1.092 (all data), R_1 = 0.0431 [8076 data with $I > 2\sigma(I)$], max/min residual electron density: +1.01/–0.79 e 10^{-6} pm^{-3}.

6: $C_{60}H_{72}N_4Rh_2$, 1055.03 g mol^{-1}, monoclinic, $P2_1/n$, a = 1429.0(3), b = 1381.4(3), c = 2699.5(5) pm, β = 99.77(3)°, V = 5251.6(19) × 10^6 pm^3, T = 200(2) K, Z = 4, μ(Mo-K_α) = 0.670 mm^{-1}, $D_{calcd.}$ = 1.334 g cm^{-3}; crystal dimensions 1.0 × 1.0 × 1.0 mm^3, 46921 reflections, 11443 unique data, R_{int} = 0.0481; 608 parameters, wR_2 = 0.1453, S = 1.038 (all data), R_1 = 0.0572 [10183 data with $I > 2\sigma(I)$], max/min residual electron density: +2.20/–2.54 e 10^{-6} pm^{-3}.

7: $C_{66}H_{92}N_4O_3Rh_2$, 1195.25 g mol^{-1}, monoclinic, $C2/c$, a = 1867.8(4), b = 1637.4(3), c = 1922.5(4) pm, β = 101.55(3)°, V = 5761(2) × 10^6 pm^3, T = 200(2) K, Z = 4, μ(Mo-K_α) = 0.622 mm^{-1}, $D_{calcd.}$ = 1.378 g cm^{-3}; crystal dimensions 0.3 × 0.1 × 0.1 mm^3, 51235 reflections, 7157 unique data, R_{int} = 0.0617; 358 parameters, wR_2 = 0.1292, S = 1.059 (all data), R_1 = 0.0455 [5435 data with $I > 2\sigma(I)$], max/min residual electron density: +0.71/–0.96 e 10^{-6} pm^{-3}.

8: $C_{42}H_{44}N_4O_4Rh_2$, 874.63 g mol^{-1}, triclinic, $P\bar{1}$, a = 896.00(18), b = 1252.0(3), c = 1878.3(4) pm, α = 74.41(3)°, β = 76.86(3)°, γ = 80.30(3)°, V = 1963.4(8) × 10^6 pm^3, T = 200(2) K, Z = 2, μ(Mo-K_α) = 0.886 mm^{-1}, $D_{calcd.}$ = 1.479 g cm^{-3}; crystal dimensions 0.4 × 0.3 × 0.2 mm^3, 35337 reflections, 9725 unique data, R_{int} = 0.0714; 482 parameters, wR_2 = 0.1131, S = 1.085 (all data), R_1 = 0.0404 [7677 data with $I > 2\sigma(I)$], max/min residual electron density: +0.75/–0.78 e 10^{-6} pm^{-3}.

Acknowledgments

Financial support by the Collaborative Research Centre CRC/Transregio 88, "Cooperative effects in homo- and heterometallic complexes (3MET)" is gratefully acknowledged (Project B4).

Keywords: N ligands · Amidinates · Rhodium · Synthesis design · Ligand effects

[1] F. T. Edelmann, *Chem. Soc. Rev.* **2012**, *41*, 7657–7672.
[2] S. Ogata, A. Mochizuki, M. Kakimoto, Y. Imai, *Bull. Chem. Soc. Jpn.* **1986**, *59*, 2171–2177.
[3] K. Dehnicke, *Chem.-Ztg.* **1990**, *114*, 295–304.
[4] F. T. Edelmann in *Adv. Organomet. Chem.* (Ed. A. F. H., M. J. Fink), Academic Press, **2008**, pp. 183–352.
[5] T. Nakane, Y. Tanioka, N. Tsukada, *Organometallics* **2015**, *34*, 1191–1196.
[6] P. C. Junk, M. L. Cole, *Chem. Commun.* **2007**, 1579–1590.
[7] M. Asay, C. Jones, M. Driess, *Chem. Rev.* **2011**, *111*, 354–396.
[8] C. Jones, *Coord. Chem. Rev.* **2010**, *254*, 1273–1289.
[9] S. P. Green, C. Jones, P. C. Junk, K.-A. Lippert, A. Stasch, *Chem. Commun.* **2006**, 3978–3980.
[10] S. Khoo, H.-X. Yeong, Y. Li, R. Ganguly, C.-W. So, *Inorg. Chem.* **2015**, *54*, 9968–9975.
[11] G.-L. Xu, M. C. DeRosa, R. J. Crutchley, T. Ren, *J. Am. Chem. Soc.* **2004**, *126*, 3728–3729.
[12] C.-W. Hsu, J.-S. K. Yu, C.-H. Yen, G.-H. Lee, Y. Wang, Y.-C. Tsai, *Angew. Chem. Int. Ed.* **2008**, *47*, 9933–9936; *Angew. Chem.* **2008**, *120*, 10081.
[13] F. T. Edelmann, *Chem. Soc. Rev.* **2009**, *38*, 2253–2268.
[14] D. Matioszek, N. Saffon, J.-M. Sotiropoulos, K. Miqueu, A. Castel, J. Escudié, *Inorg. Chem.* **2012**, *51*, 11716–11721.
[15] F. J. Lahoz, A. Tiripicchio, M. T. Camellini, L. A. Oro, M. T. Pinillos, *J. Chem. Soc., Dalton Trans.* **1985**, 1487.
[16] C. Jones, D. P. Mills, A. Stasch, *Dalton Trans.* **2008**, 4799–4804.
[17] J. R. Hagadorn, J. Arnold, *J. Organomet. Chem.* **2001**, *637–639*, 521–530.
[18] D. Chartrand, G. S. Hanan, *J. Phys. Chem. A* **2014**, *118*, 10340–10352.
[19] M. B. Hursthouse, M. A. Mazid, T. Clark, S. D. Robinson, *Polyhedron* **1993**, *12*, 563–565.
[20] Selected examples: a) Y. Lei, F. Chen, Y. Luo, P. Xu, Y. Wang, Y. Zhang, *Inorg. Chim. Acta* **2011**, *368*, 179–186; b) J. Grundy, M. P. Coles, P. B. Hitchcock, *New J. Chem.* **2004**, *28*, 1195; c) W. Zhang, L. R. Sita, *Adv. Synth. Catal.* **2008**, *350*, 439.
[21] D. Walther, T. Döhler, N. Theyssen, H. Görls, *Eur. J. Inorg. Chem.* **2001**, 2049–2060.
[22] J. Yang, P. Xu, Y. Luo, *Chin. J. Chem.* **2010**, *28*, 457–462.
[23] P. Fehling, M. Döring, F. Knoch, R. Beckert, H. Görls, *Chem. Ber.* **1995**, *128*, 405–412.
[24] T. Döhler, H. Görls, D. Walther, *Chem. Commun.* **2000**, 945–946.
[25] S.-H. Chi, Y.-J. Luo, J. Chen, *Synth. React. Inorg. Met.-Org. Nano-Met. Chem.* **2014**, *44*, 611–615.
[26] N. Kazeminejad, D. Munzel, M. T. Gamer, P. W. Roesky, *Chem. Commun.* **2017**, *53*, 1060–1063.
[27] M. L. Cole, A. J. Davies, C. Jones, P. C. Junk, *J. Organomet. Chem.* **2004**, *689*, 3093–3107.
[28] Y.-Y. Zhang, Y.-J. Lin, G.-X. Jin, *Chem. Commun.* **2014**, *50*, 2327–2329.
[29] M. Li, J. Hong, Z. Chen, X. Zhou, L. Zhang, *Dalton Trans.* **2013**, *42*, 8288–8297.
[30] K. Ookawa, J. Abe, T. Taie, T. Watanabe, K. Fujimoto, M. Kuramoto, *Substituted Bisamidino Compounds*, **n. d.**, JP 46002803.
[31] K. F. Kalz, A. Hausmann, S. Dechert, S. Meyer, M. John, F. Meyer, *Chem. Eur. J.* **2016**, *22*, 18190–18196.
[32] R. Bauer, *Ber. Dtsch. Chem. Ges.* **1907**, *40*, 2650–2662.
[33] E. J. Baran, *J. Coord. Chem.* **2014**, *67*, 3734–3768.
[34] S. Rau, K. Lamm, H. Görls, J. Schöffel, D. Walther, *J. Organomet. Chem.* **2004**, *689*, 3582–3592.
[35] Y.-H. Wen, X.-M. Li, L. Wang, S.-S. Zhang, *Acta Crystallogr., Sect. E Struct. Rep. Online* **2006**, *62*, o2185–o2186.
[36] J. P. Rourke, G. Stringer, P. Chow, R. J. Deeth, D. S. Yufit, J. A. K. Howard, T. B. Marder, *Organometallics* **2002**, *21*, 429–437.
[37] M. J. Cowley, J. M. Lynam, J. M. Slattery, *Dalton Trans.* **2008**, 4552–4554.
[38] Recent contributions from our laboratory: a) A. Feyrer, M. K. Armbruster, K. Fink, F. Breher, *Chem. Eur. J.* **2017**, *23*, 7402–7408; b) A. Feyrer, F. Breher, *Inorg. Chem. Front.* **2017**, *4*, 1125–1134; c) F. Walz, E. Moos, D. Garnier, R. Köppe, C. E. Anson, F. Breher, *Chem. Eur. J.* **2017**, *23*, 1173–1186; General reviews: d) J. R. Khusnutdinova, D. Milstein, *Angew. Chem. Int. Ed.* **2015**, *54*, 12236; *Angew. Chem.* **2015**, *127*, 12406; e) J. I. van der Vlugt, *Eur. J. Inorg. Chem.* **2012**, 363; f) J. Park, S. Hong, *Chem. Soc. Rev.* **2012**, *41*, 6931; g) I. Bratko, M. Gómez, *Dalton Trans.* **2013**, *42*, 10664; h) P. Buchwalter, J. Rosé, P. Braunstein, *Chem. Rev.* **2015**, *115*, 28; i) J. A. Mata, F. E. Hahn, E. Peris, *Chem. Sci.* **2014**, *5*, 1723; j) P. J. Chirik, *Inorg. Chem.* **2011**,

© 0000 Wiley-VCH Verlag GmbH & Co. KGaA, Weinheim

50, 9737; k) V. Lyaskovskyy, B. de Bruin, *ACS Catal.* **2012**, *2*, 270; l) A. M. Allgeier, C. A. Mirkin, *Angew. Chem. Int. Ed.* **1998**, *37*, 894; *Angew. Chem.* **1998**, *110*, 936; m) O. R. Luca, C. H. Crabtree, *Chem. Soc. Rev.* **2013**, *42*, 1440; n) V. K. K. Praneeth, M. R. Ringenberg, T. R. Ward, *Angew. Chem. Int. Ed.* **2012**, *51*, 10228; *Angew. Chem.* **2012**, *124*, 10374; o) V. Blanco, D. A. Leigh, V. Marcos, *Chem. Soc. Rev.* **2015**, *44*, 5341.

[39] M. Findlater, N. J. Hill, A. H. Cowley, *Dalton Trans.* **2008**, 4419–4423.

[40] a) G. M. Sheldrick, *Acta Crystallogr., Sect. A* **2015**, *71*, 3; b) G. M. Sheldrick, *Acta Crystallogr., Sect. C* **2015**, *71*, 3.

[41] T. Hahn, *International Tables for Crystallography – Volume A*, 5th ed., Kluwer Acad. Publ., Dordrecht **2002**.

Received: March 16, 2018

© 0000 Wiley-VCH Verlag GmbH & Co. KGaA, Weinheim

Tuning M–M Distances

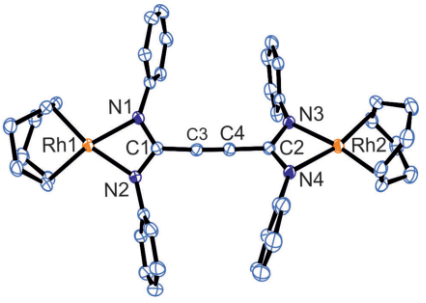

The first mono- and dinuclear rhodium(I) complexes based on amidinates, oxalamidinates, and linker-bridged bis(amidinates) are reported. The compounds were obtained by salt metathesis reactions of the alkali metal salts of the chelating N donor ligands and have been fully characterized by various methods.

https://doi.org/10.1002/ejic.201800349

 © 0000 Wiley-VCH Verlag GmbH & Co. KGaA, Weinheim